Received: 13 December 2022 | Accepted: 18 April 2023

DOI: 10.1111/imm.13654

ORIGINAL ARTICLE

immunology
Insights into immunity in health and disease

CD83$^+$ B cells alleviate uveitis through inhibiting DCs by sCD83

Meng Feng[1,2,3] | **Xin Wang**[4,5] | **Shuping Zhou**[1,2,3] | **Minghao Li**[1,2,3] | **Tingting Liu**[6] | **Xunbin Wei**[7,8,9,10,11] | **Wei Lin**[1,2,3]

[1]Department of Rheumatology and Autoimmunology, The First Affiliated Hospital of Shandong First Medical University & Shandong Provincial Qianfoshan Hospital, Jinan, China

[2]School of Clinical and Basic Medicine, Shandong First Medical University &Shandong Academy of Medical Sciences, Jinan, China

[3]Shandong Key Laboratory of Rheumatic Disease and Translational Medicine, Shandong Medicine and Health Key Laboratory of Rheumatism, The First Affiliated Hospital of Shandong First Medical University, Jinan, China

[4]Department of Clinical Laboratory, Qilu Hospital, Shandong University, Jinan, China

[5]Shandong Engineering Research Center of Biomarker and Artificial Intelligence Application, Jinan, China

[6]Shandong Eye Hospital, State Key Laboratory Cultivation Base, Shandong Provincial Key Laboratory of Ophthalmology, Shandong Eye Institute, Shandong First Medical University & Shandong Academy of Medical Sciences, Jinan, China

[7]Biomedical Engineering Department, Peking University, Beijing, China

[8]School of Biomedical Engineering, Anhui Medical University, Hefei, China

[9]Institute of Medical Technology, Peking University Health Science Center, Beijing, China

[10]Key Laboratory of Carcinogenesis and Translational Research (Ministry of Education/Beijing), Peking University Cancer Hospital & Institute, Beijing, China

[11]International Cancer Institute, Peking University, Beijing, China

Correspondence
Wei Lin, School of Clinical and Basic Medicine, Shandong First Medical University &Shandong Academy of Medical Sciences, Jinan, 250062, China.
Email: linw1978@163.com

Tingting Liu, Shandong Eye Hospital, State Key Laboratory Cultivation Base, Shandong Provincial Key Laboratory of Ophthalmology, Shandong Eye Institute, Shandong First Medical University & Shandong Academy of Medical Sciences, Jinan, 250000, China.
Email: tingtingliu@vip.sina.com

Xunbin Wei, Biomedical Engineering Department, Peking University, Beijing 100081, China.
Email: xwei@bjmu.edu.cn

Funding information
National Natural Science Foundation of China, Grant/Award Numbers: 81500710, 81601757; projects of medical and health

Abstract

Soluble CD83 (sCD83) exerts immunosuppressive functions in many autoimmune diseases, including experimental autoimmune uveitis (EAU), but the cells and mechanisms involved are unclear. This study showed that CD83$^+$ B cells were the main sources of sCD83. They alleviated the symptoms of EAU and decreased the percentage of T cells and DCs in the eyes and lymph nodes. These CD83$^+$ B cells decreased IL-1β, IL-18 and IFN-γ secretion by DCs through sCD83. sCD83 interacted with GTPase Ras-related protein (Rab1a) in DCs to promote Rab1a accumulation in autolysosomes and inhibit mTORC1 phosphorylation and NLRP3 expression. Hence, CD83$^+$ B cells play a regulatory role in EAU by secreting sCD83. The lack of regulation of CD83$^+$ B cells might be an important factor leading to hyperimmune activation in patients with autoimmune uveitis. CD83$^+$ B cells suppress activated DCs in uveitis, indicating the potential therapeutic role of CD83$^+$ B cells in uveitis.

KEYWORDS
autoimmune uveitis, CD83$^+$ B cells, DCs, immunoregulation, Rab1a, sCD83

Meng Feng, Xin Wang and Shuping Zhou are co-first authors.

technology development program in Shandong province, Grant/Award Number: 2019WS186; Shandong Key Research and Development Project, Grant/Award Number: 2019GSF108189; the Innovation Project of Shandong Academy of Medical Sciences

INTRODUCTION

Autoimmune uveitis (AIU) is an organ-specific disorder characterized by immune disorders, including increased CD4$^+$ T cell infiltration in the eyes [1–3], and can cause visual deficits and blindness [4]. Type 1 helper T cells (Th1) are crucial effectors that drive local tissue damage and systemic progression [3]. Dendritic cells (DCs) are antigen-presenting cells and are involved in T cell activation and the pathogenic process underlying uveitis by secreting interleukin (IL)-18 and IL-1β [5–9]. Still, little is known about the reason for the abnormal activation of T cells and DCs in AIU. One of the important reasons for the over-activation of immune cells is the lacking of inhibitory molecules or cells in this disease, for example, regulatory B cells (Bregs), which are important regulators in autoimmune diseases [10, 11]. Bregs negatively regulate immune responses through the production of anti-inflammatory cytokines such as IL-10, IL-35 and TGF-β, and they exhibit various mechanisms of immunosuppression in autoimmune diseases [10, 11].

Soluble CD83 (sCD83) is increased during EAU and inhibits the activation of T cells by suppressing DC activation [12]. sCD83 is the extracellular domain of the membrane-bound CD83 (mCD83) molecule, a suppressive factor for many autoimmune diseases [13–15]. Therefore, the source of sCD83 might be an important clue for suppressing the immune response of uveitis. sCD83 has been reported to be mainly produced by CD83-positive cells, including CD83$^+$ B cells and CD83$^+$ DCs [16], but which cell subset is the main source of sCD83 in EAU is unknown. The overexpression of CD83 in mouse B cells leads to function inhibition, as demonstrated by a decreased capacity of proliferation, immunoglobulin (Ig) class-switch, Ig secretion upon immunization and augmented secretion of the immunoregulatory cytokine IL-10 [17, 18]. Whether CD83$^+$ B cells is the main source of sCD83 in EAU and its role in immunoregulation are not clear.

Although it has been reported that sCD83 induces DC tolerance and regulates DC status [12, 19, 20], the target and the possible mechanisms of sCD83 in DCs are still unclear. Moreover, our previous reports showed that sCD83 inhibited mature DCs by changing the localization of mitochondria and decreased calcium signalling in DCs [12], suggesting that sCD83 might affect the metabolism of DCs. The reprogramming of the intracellular metabolic pathways was speculated to regulate the activation and effector function of DCs [21, 22]. Blocking glycolysis or mitochondria metabolism inhibits the activation and secretion of inflammatory factors of DCs [23–25]. The metabolism of DCs is primarily regulated by mTORC1 and its signalling pathways [26, 27], which might be correlated with the occurrence of uveitis [28].

In our study, the EAU mice model was used to investigate the source of sCD83 and the putative mechanisms underlying the effects of sCD83 on DCs and T cells. Subsequently, the role of sCD83 and CD83$^+$ B cells in patients with uveitis was investigated.

MATERIALS AND METHODS

Animals and experimental autoimmune uveitis (EAU) model

Pathogen-free female C57BL/6 (6–8 weeks) mice were purchased from the Beijing Vital River Laboratory Animal Technology Co., Ltd. μMT mice (Ighm-eKO1) were purchased from the Jackson Laboratory (Bar Harbour). These mice were maintained in specific pathogen-free conditions as per the guidelines for the care and use of laboratory animals of the Shandong First University & Shandong Academy of Medical Sciences. The induction of EAU in C57BL/6 mice was described in a previous report [29–31]. Briefly, the C57BL/6 mice were subcutaneously immunized with 350 μg of human interphotoreceptor retinoid-binding protein peptide $_{1–20}$ (IRBP$_{1–20,}$ China Peptides Co., Ltd.) that was emulsified in complete Freund's adjuvant (Sigma-Aldrich Company). Concurrently, a single dose of 500 ng of pertussis toxin (PTX, Enzo Life Sciences) was injected intraperitoneally. After immunization for 21 days, the mice were examined by histopathological examination and the degree of disease was evaluated by a scoring system as previously described [31, 32]. For DCs depletion, CD11c-DTR-GFP mice was immunized to construct EAU model, after 16 days, diphtheria toxin (DT, 5 ng/eye) was used to delete the CD11c cells in the eyes of CD11c-DTR-GFP mice by subconjunctival injection [5, 33]. This approach resulted in 95% depletion of CD11c cells and lasted for 72 h [5, 33]. Mouse/human IL-1β, IL-18, IFN-γ ELISA kits (eBioscience) were used for cytokines detection in serum.

Cell culture

The DC2.4 cell line (a gift from Professor Yiwei Chu of the Department of Immunology, Shanghai Medical School, Fudan University) was cultured in RPMI-1640 containing 10% fetal bovine serum and double antibodies. These cells were stimulated overnight with IRBP1-20 (10 ng/mL) and PTX (10 ng/mL).

The $CD83^+$ $CD3^-$ $CD19^+$ B cells were isolated from the lymph nodes of EAU mice by a cell sorting instrument (BD FACS Aria™ III, BD Biosciences). These cells (1×10^6/100 μL/mouse) were injected into the EAU mice and immunized after 16 days via the tail vein. For cell stimulation, these $CD83^+$ B cells were treated with either 10 μg/mL LPS for 48 h or 50 ng/mL PMA and 500 ng/mL ionomycin for the last 5 h. In order to examine the effect of antigens on $CD3^-$ $CD19^+$ B cells, the cells were stimulated with anti-CD40 mAb (50 ng/mL; FGK4.5, BioXcell), $IRBP_{1\text{-}20}$ (10 ng/mL) and PTX (10 ng/mL). Subsequently, the cells were used for flow cytometry. Afterward, the $CD83^+$ B cells were added into the culture of DCs (B cell: DC_m = 1:1) or DCs and T cells (T cell: DC_m: B cell = 10:1:1) for 24–48 h.

For cell stimulation, sCD83 (100 ng/mL) was added to the culture of isolated wild-type (WT) DCs or the DC2.4 cell line or isolated B cells for pre-treatment for 24 h, and then the cells were collected for detection.

Plasmid construction

The mouse pGEM-T-sCD83 plasmid (the extracellular domain of mCD83 molecule, 22–133) was purchased from Sino Biological Inc. and inserted into pGEX4T-1 using BamHI and XhoI restriction enzymes to construct pGEX 4 T-1-sCD83 for sCD83 protein expression. The genes of sCD83 and Rab1A (Sino Biological Inc.) were constructed into pEYFP-N1 and pCFP-C1 to make p-sCD83-EYFP and p-Rab1a-CFP, respectively. $Rab1a^{Q70L}$ (a GTP-restricted mutant, activated form), $Rab1a^{S25N}$ (a GDP-restricted mutant, inactivated form) and $Rab1a^{N124I}$ (dominant-negative guanine nucleotide binding-deficient mutant) were generated by PCR site-directed mutagenesis and confirmed by sequencing (Shanghai Biosune Biotechnology Co.). The plasmids for mTOR and NLRP3 were purchased from Hunan Fenghui Biotechnology Co., Ltd. These plasmids were transfected into the DC2.4 cells using Lipofectamine 2000 (Thermo Fisher Scientific).

Non-targeting control shRNA and targeting shRNA were constructed by Genomeditech Company. The sequence of effective Rab1a shRNA was 5′-GCACAATTGGTGTG-GATTT-3′, and the sequence of CD83 shRNA was 5′-GUGCUUUUCAGUCAUCUACAAGCTA-3′. They were constructed into PGMLV-SC5 separately. The cells were then transfected with 5–20 nM PGMLV-SC5-Rab1a shRNA/PGMLV-SC5-CD83 shRNA or non-targeting control shRNA (NC) as per the protocol provided by the manufacturer.

Cell depletion

In order to determine which cells produced sCD83, $CD45^+$ $CD83^+$ cells were obtained from lymph nodes using a cell sorting instrument (BD FACSAria™ III, BD Biosciences), after which CD19 depletion was performed using mouse CD19 MicroBeads (Miltenyi Biotec GmbH). For CD4 depletion, a negative selection mouse $CD4^+$ T Cell Isolation kit (Miltenyi Biotec GmbH) was used, while CD11c depletion was done using mouse CD11c MicroBeads (Miltenyi Biotec GmbH). Cells (1×10^5) of every group were obtained and cultured with 250 μL RPMI-1640 culture medium and stimulated with $IRBP_{1\text{-}20}$ (10 ng/mL) and PTX (10 ng/mL) as described above.

Flow cytometry and cell sorting

Wild-type (WT) DCs and $CD4^+$ T cells were obtained from the lymph node of EAU mice and selected using a CD4-nagetive and CD11c-positive selection kit (Miltenyi Biotec), respectively. Splenocytes were obtained, and the Red Blood Cell Lysis Buffer (Solarbio Science & Technology Co., Ltd.) was used to obtain a single-cell suspension. Aliquots of 1×10^6 cells were stained with different monoclonal antibodies according to standard protocols. The cells were analysed on a FACS Verse cytometer (BD Biosciences). Fluorescent antibodies against mouse CD45 (clone 30-F-11), mouse CD3ε (clone 145-2C11), CD4 (clone GK1.5), mouse CD83 (clone Michel-19), mouse CD19 (clone eBio103), mouse NK1.1 (clone PK136), mouse MHC-II (clone M5/114.15.2), mouse CD11c (clone N418), mouse CD69 (clone H1.2F3), mouse Ki67 (clone B56), mouse CD80 (clone 16-10A1), mouse CD86 (clone GL-1), mouse IL-10 (clone 7ES5-16E3), mouse IL-35 (IL-12p35) (clone 45 806), mouse IFN-γ (clone XMG1.2), human CD45 (clone ID1), human CD3 (clone HIT3a), human CD19 (clone HIB19), human CD83 (clone HB15e), human IL-35 (clone B032F6) and human IL-10 (clone JES-9D7) conjugated with the corresponding fluorescent dyes (eBioscience), and mouse NLRP3 (clone #768319) from R&D Systems Inc. or Biolegend were used in the experiments.

Immunofluorescence

Wild-type DCs or DC2.4 cells were incubated with $IRBP_{1\text{-}20}$ (10 ng/mL) and PTX (10 ng/mL) overnight.

sCD83 (100 ng/mL) was added to stimulate the cells overnight. The cells were fixed in PBS/4% paraformaldehyde for 10 min, followed by incubation with PBS/0.1 M of glycine for 3 min. The cells were punctured with 0.1% Triton X-100/PBS for 20 min and then blocked with 2% bovine serum albumin buffer for 20 min. The cells were stained with anti-Rab1a, p-mTORC1, LC3, LAMP1 and GM130 antibodies (1:1000 dilution) for 60 min. After washing three times, the corresponding fluorescent antibodies were added. Images of the cells were taken with a confocal microscope (LMS 880, Zeiss, Germany) equipped with an APO oil immersion objective lens (63×, NA = 1.40). The images were analysed with the Imaris Software (Bitplane AG) and ImageJ (National Institutes of Health). Colocalization of Rab1a and GM130, LAMP1 and LC3 in DCs were analysed by ImageJ with colocalization index (Pearson correlation coefficient, Pearson's *r*).

GST-pulldown and liquid chromatographic tandem mass spectrometry detection

The purified GST-CD83 protein (200 μg) was incubated with GSH-coupled agarose beads (Thermo Fisher Scientific) in 300 μL of binding buffer (20 mM imidazole, 10% glycerol, and 500 mM NaCl, pH 7.9) containing protease inhibitor at 4°C. The DC membrane proteins were extracted, washed once with 800 μL of PBS + 1% Triton-100, and co-incubated with GST-CD83 at 4°C overnight. The complex of GSH-coupled agarose beads and GST-CD83 and membrane protein extraction were identified by SDS-PAGE and western blot. The sample was digested using 40 μL of trypsin buffer, desalted, separated by capillary high-performance liquid chromatography and analysed using a Q Exactive mass spectrometer. The identified proteins were analysed using the mascot 2.2 software. Liquid chromatographic tandem mass spectrometry was performed by DetaiBio Company.

Western blot

The DC2.4 cells or sCD83-treated-DC2.4 cells were lysed with RIPA buffer (Beyotime Biotechnology, Shanghai, China). The same amounts of proteins were separated by 10% SDS-PAGE and transferred to polyvinylidene difluoride (PVDF) membranes. Subsequently, 5% non-fat dry milk in Tris-buffered saline 0.1% Tween 20 (TBS-T) was used to block the non-specific binding sites for 1 h. After washing with TBS-T, the membranes were incubated with primary antibodies (1:1000) against mouse Rab1a, mTORC1, p-mTORC1 and β-actin (Cell Signalling Technology) at 4°C overnight. The membranes were washed and incubated with secondary goat-anti-rabbit IgG antibodies conjugated with HRP (Beyotime Biotechnology) for 1 h. Finally, the membranes were developed using the Super Signal West pico Chemiluminescent Substrate (Thermo Scientific). Densitometric analyses were performed using the Image J software (National Institutes of Health).

Single-cell RNA-sequencing analysis

The original data of the YN_10 × RNA and YE_10 × RNA groups were downloaded from the CRA004687 dataset of the Genome Sequence Archive (GSA) [34]. 'CellRanger count' of cellranger 3.1.0 in Linux Environment was used to analyse multiplex and process the FastQ sequence in the NovaSeq system, and Seurat software (version 2.3.4) was used for filtering, data standardization, dimensionality reduction, clustering, and the single cell expression matrix analyse [35]. The Rstudio software was used to carry out quality control and dimensionality reduction of data and data analysis. The following parameters were assessed. (1) Including features detected in at least three cells. (2) Including detecting at least 200 features in each cell. (3) Before proceeding further, cells with <200 or >2500 genes or with a ratio of mitochondrial genes >15% were excluded. Most cells with high expression of Hbb-a1 and Hbb-bs that were recognized as red blood cells were filtered. The batch effect across different samples was removed. For the analysis of scRNA-seq data with Seurat, the data were normalized using the 'NormalizeData' function with the 'SCT'. In addition, the 'FindClusters' function was used to cluster cells, and the 'RunUMAP' function was used to visualize with a 2-dimensional UMAP algorithm. The 'FeaturePlot' parameter was used to visualize the expression of CD83 in each cell subgroup.

Patient's samples and cell isolation

This study was approved by the Human Research and Ethics Committee of Shandong Eye Hospital, Shandong Eye Institute, Shandong First Medical University and Shandong Academy of Medical School (2019-G-012). All patients provided written informed consent. A total of 15 patients with uveitis due to Behcet's disease (BD) and 15 patients with acute uveitis were recruited from the Shandong ophthalmic hospital from September 2019 to July 2021. Uveitis of BD was diagnosed based on the criteria from the international diagnostic standard in 2014 [36]. Acute uveitis was diagnosed in patients who had no history of uveitis in the past, and the duration of this

medical history was ≤ 3 months. The healthy controls were from the health examination personnel of Qilu Hospital of Shandong University, all without eye disease. Serum samples were obtained to detect the concentration of IL-10, IL-35 and sCD83 using the human IL-10, IL-35 and sCD83 ELISA Kits (USCN Life Science Inc.). Heparinized venous blood (2 mL) was obtained from patients and healthy controls. Peripheral blood mononuclear cells (PBMCs) were recovered at the buffy coat layer using a Ficoll–Hypaque (Beijing Solarbio Science & Technology Co., Ltd.) gradient and then washed twice to remove red blood cells (RBCs). The phenotypic analysis of fresh PBMCs was performed by flow cytometry.

Statistical analysis

Data analysis was performed using GraphPad Prism 5 (GraphPad Software). Data were analysed by the two-tailed Student's *t*-test or one-way ANOVA. The data were presented as mean ± SEM, *p*-values < 0.05 (*), 0.01 (**), or 0.001 (***) were considered significant, and *p*-values > 0.05 (N) was considered not significant.

RESULTS

$CD83^+$ B cells are the main cell subset for sCD83 secretion in EAU

The expression of CD83 in various cell subsets from lymph nodes of WT and EAU mice was analysed by single-cell sequencing data from previously report [34]. The integrated samples were grouped and defined as 11 cell subpopulations, including precursor T cells (pro-T), $CD4^+$ T cells, $CD8^+$ T cells, Tregs, B cells, plasma cells, neutrophils, monocyte cells, macrophage cells, cDCs and pDCs (Figure S1, left panel). The subset of B cells was divided into three subsets (Figure S1, middle panel), and the subset that highly expressed CD83 was specifically overexpressing *CD83, Fcmr, Il4i1* and *CD72*. According to the expression of CD83, we redefined the subgroup of B cells with high expression of CD83 into $CD83^+$ B cells and $CD83^-$ B cell clusters, as shown in Figure S1 (right panel).

It was found that the expression of CD83 in B cells was significantly higher than that in all other cell subsets (Figure 1a) and the expression of CD83 in B cells from EAU, was higher than that from WT mice (Figure S1), suggesting that the secretion of CD83 in EAU might mainly come from B cells. Furthermore, the $CD83^+$ $CD45^+$ cell subsets from the lymph nodes of EAU mice were isolated and analysed by flow cytometry. The $CD83^+$ $CD3^-$ $CD19^+$ B cells were the major component (Figures 1b and S1). Furthermore, the concentration of sCD83 was detected in the supernatant of isolated $CD83^+$ $CD45^+$ cells from the lymph nodes of EAU mice, as well as the $CD83^+$ $CD45^+$ cell pool with depleting $CD11c^+$ $MHC\text{-}II^+$ DCs, $CD3^-$ $CD19^+$ B cells or $CD3^+$ T cells, respectively. The concentration of sCD83 in the medium was reduced to different degrees after the depletion of different cell subsets (Figure 1c). Specifically, the concentration of sCD83 in the medium of cells with $CD3^-$ $CD19^+$ B cells depletion decreased notably (Figure 1c). There were no significant differences in the concentration of sCD83 between the medium of $CD83^+$ $CD3^-$ $CD19^+$ B cells and $CD45^+$ $CD83^+$ cells (Figure S2). This phenomenon indicated that $CD83^+$ B cells are the main cell subset to produce sCD83. In order to detect the secretion of sCD83 by $CD83^+$ B cells in vivo, the $CD83^+$ B cells were transferred into EAU to increase the concentration of sCD83 in the serum of the transferred mice (Figure 1d). Furthermore, the $EAU^{\mu MT}$ mice models were established using μMT mice (B cell function-deficient mice) to detect whether the loss of B cells affects the secretion of sCD83 in vivo. The concentration of sCD83 in the serum of $EAU^{\mu MT}$ mice was lower than in the EAU mice (Figure 1d). The concentration of sCD83 increased after $CD83^+$ B cells were transferred into $EAU^{\mu MT}$ mice (Figure 1d). These data showed that $CD83^+$ B cells are the main sCD83-secreting cells.

The total ocular B cells peaked in the initial stages of inflammation (8–12 days) and peaked a second time at 20–24 days during the process of EAU (Figure 1e). The percentage of $CD83^+$ B cells increased and peaked on day 28. The concentration of sCD83 in the serum increased and peaked on day 32, which was the recovery stage of EAU (Figure 1e,f). In addition, 14.7% of the B cells from the eyes with EAU were $CD83^+$ B cells (Figure 1g), which might be the main source of sCD83 in the eyes. These data indicated that the increased sCD83 concentration in EAU was correlated with $CD83^+$ B cells.

Subsequently, an in vitro experiment showed that $IRBP_{1\text{-}20}$ and PTX promoted B cells to express a high level of CD83 on the B cell surface (Figure S3), revealing that $CD83^+$ B cells were stimulated by antigen peptide and PTX.

$CD83^+$ B cells play a regulatory role in EAU by suppressing DCs and T cells

The gene expression levels of B cell activation markers *CD40, CD86*, *CD83* and the gene of major histocompatibility complex 2 (*MHC-II*), including *H2-Aa, H2-D1, H2-Ab1, H2-K1*, *H2-Eb1* and *CD74* in $CD83^+$ B cells were higher than on $CD83^-$ B cell (Figure 2a). *EBI3*, a subunit

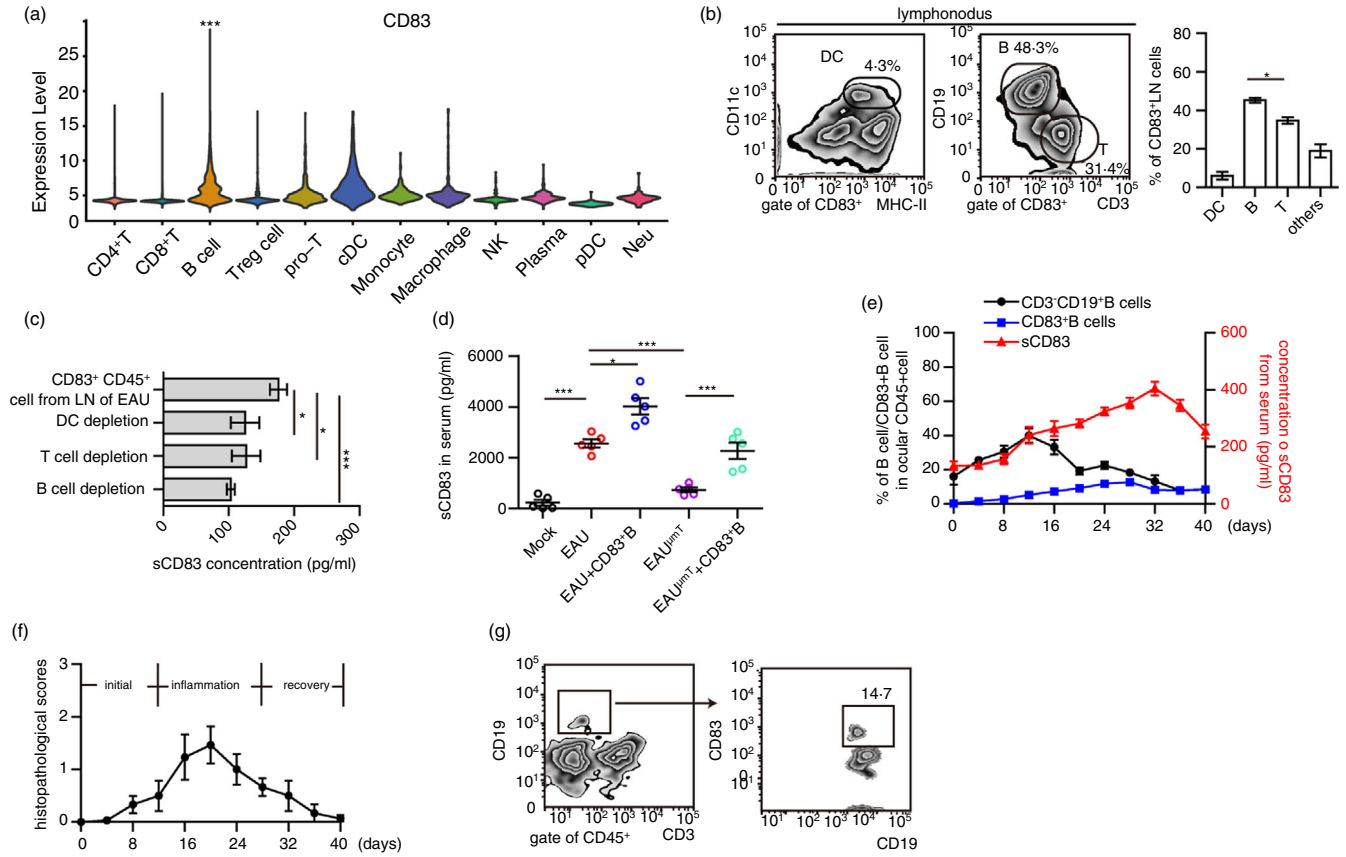

FIGURE 1 sCD83 were secreted by CD83$^+$ B cells in EAU. (a) CD83 positive subsets in lymph nodes (LNs) were analysed by Single-cell RNA-sequencing analysis (The statistics of B cells are statistically significant differences compared to all other cell populations, one-way ANOVA, ***$p < 0.001$). (b) The percentage of CD83$^+$ CD11c$^+$ MHC-II$^+$ (CD83$^+$DCs), CD83$^+$ CD3$^-$ CD19$^+$ (CD83$^+$ B cells), CD83$^+$ CD3$^+$ (CD83$^+$T cells) and others in the CD83$^+$ leukocytes from the LNs of EAU mice. (c) The concentration of sCD83 in the supernatant of isolated leukocytes from the LNs of EAU with CD3$^+$T cells, CD11c$^+$ DC or CD19$^+$ B cells depletion separately or not. (d) The concentration of sCD83 in the serum of EAU, EAU with CD83$^+$ B cells transferring, EAU$^{\mu mT}$, EAU$^{\mu mT}$ with CD83$^+$ B cells transferring mice model. (b–d) $n = 5$/group. mean ± SEM one-way ANOVA, *$p < 0.05$, *** $p < 0.001$. (e) The dynamic changes of the percentage of CD3$^-$ CD19$^+$ B cells and CD83$^+$ CD3$^-$ CD19$^+$ B cells from the eyes of EAU. (f) The histopathological severity score in the eyes of EAU mice over time. (e, f) each point represents 3/time point in triplicates, mean ± SEM) (g) The percentage of ocular CD83$^+$ B cell of EAU mice. The experiment was repeated three times (33.2 ± 21.1, 23.9 ± 10.5, 14.7 ± 4.5), and the representative result of one of the experiments was shown.

of inhibitory factor IL-35, in CD83$^+$ B cells were higher than on CD83$^-$ B cell (Figure 2a). Although the gene expression of IL-10 is not changed between CD83$^+$ B cells and CD83$^-$ B cells, the protein expression of IL-10 is increased in CD83$^+$ B cells (Figure 2a,c). Similarly, the protein expression levels of CD40, CD86, IL-35 (IL-12p35) and MHC-II of CD83$^+$ B cells in lymph nodes were higher than on CD83$^-$ B cells by flow cytometry (Figure 2b,c). However, when a specific shRNA-CD83 was used to knock down CD83 expression in CD83$^+$ B cells, the expression levels of CD83 and the secretion of sCD83, IL-10 and IL-35 were reduced (Figure S4a–c). Thus, CD83 expression in B cells might control the regulatory function of the B cells.

The symptoms of EAU mice were lessened after CD83$^+$ B cell transferring (Figure 2d). The EAU model of B cell-deficient μMT mice also showed severe retinal injury and immune inflammatory response, suggesting that lacking B cells leads to a deficient regulatory function in EAU. Transferring CD83$^+$ B cells also lessened the symptom of retinal damage in EAU$^{\mu MT}$ mice models (Figure 2d). These data showed that CD83$^+$ B cells played a regulatory role in EAU. In addition, the effects of CD83$^+$ B cells on various subsets of lymphocytes were detected. After CD83$^+$ B cell transfer, the ratio and the quantity of CD11c$^+$ MHC-II$^+$ DCs and CD3$^+$ T cells in the eyes and lymph nodes of EAU mice decreased compared with EAU mice without transfer and EAU$^{\mu MT}$ mice models (Figures 2e,f and S5a,b). Moreover, CD83$^+$ B cells transfer also decreased the percentage of CD4$^+$ IFN-γ$^+$ T cells in EAU (Figures 2g and S5c) and decreased the concentration of IL-1β, IL-18 and IFN-γ in the serum of

EAU, and the percentage of DCs expressed IL-1β, IL-18 and IFN-γ (Figure 2h,i). Thus, the CD83$^+$ B cells might be a regulator in EAU by suppressing DCs and T cells.

In order to analyse the role of CD83$^+$ B cells on DCs and T cells, CD83$^+$ B cells were cocultured with CD3$^+$ T cells in vitro, and CD83$^+$ B cells directly decreased the activation

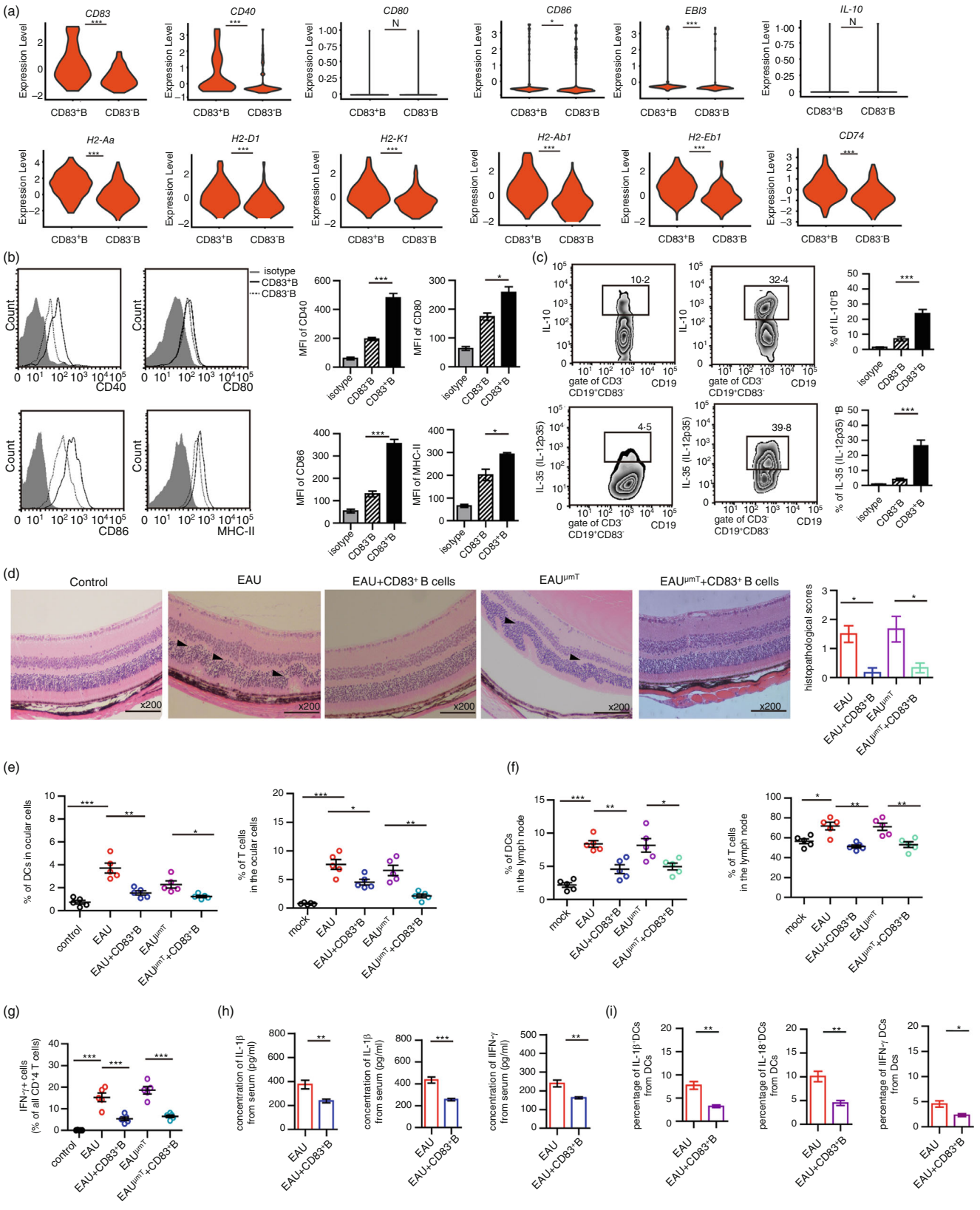

FIGURE 2 Legend on next page.

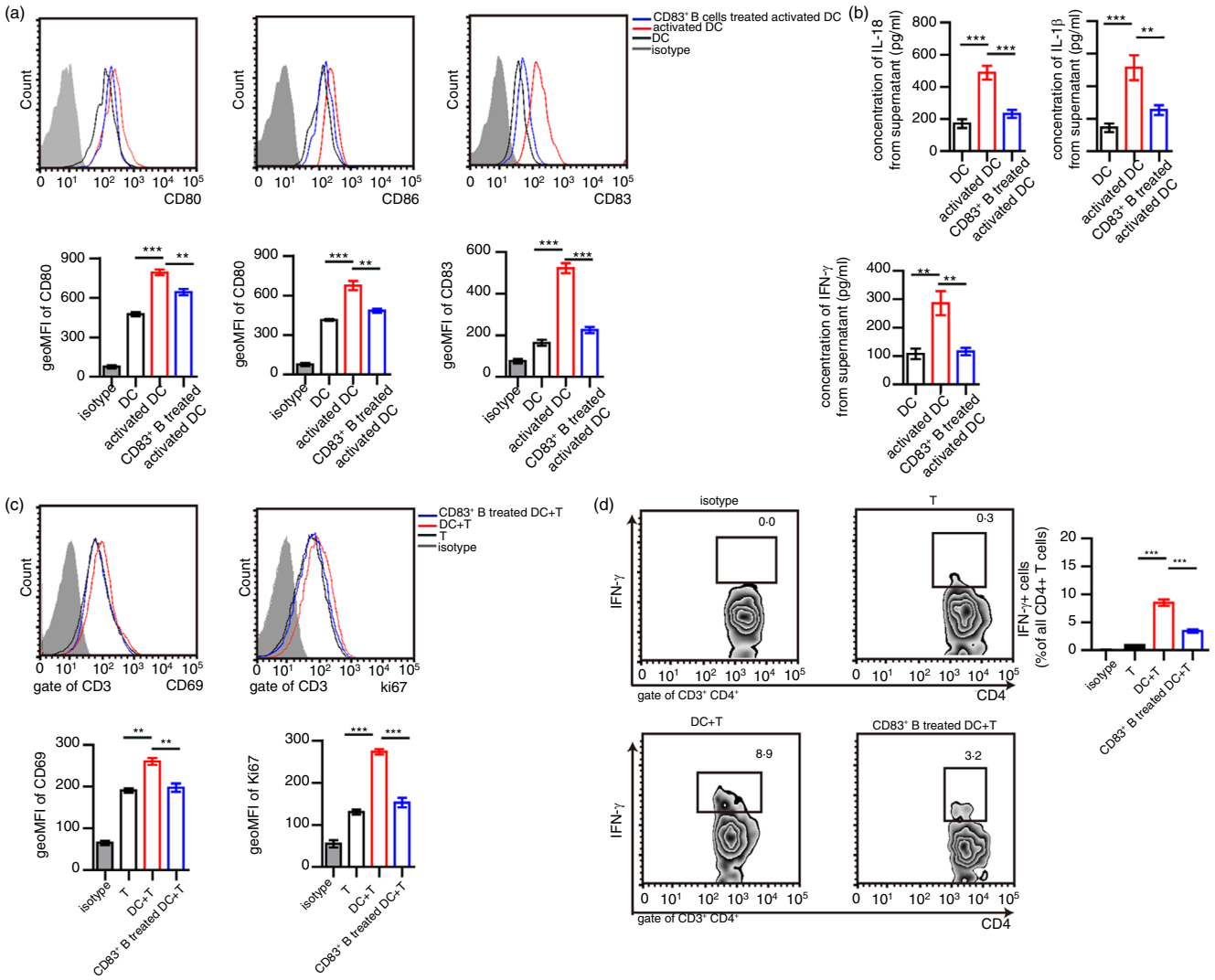

FIGURE 3 CD83$^+$ B cells suppressed the activation, pro-inflammatory factors secretion and function of DCs. (a) The expression of CD80, CD86 and CD83 on DCs, IRBP and PTX stimulated activated DCs and CD83$^+$ B-treated-activated-DCs. (b) The concentration of IL-1β, IL-18 and IFN-γ from the supernatant of DCs, DCs with IRBP and PTX stimulation (activated DCs), or CD83$^+$ B cells treated activated DCs. (c) The expression of CD69 and Ki67 in CD3$^+$T cells cocultured with or without activated DCs, or CD83$^+$ B-treated-activated-DCs. (d) The percentage of IFN-γ$^+$ cells in CD4$^+$T cells which contact with activated DCs, or CD83$^+$ B-treated activated DCs, or not. Data of (a–d) are from three separate experiments and shown as mean ± SEM, one-way ANOVA, $^*p < 0.05$, $^{**}p < 0.01$, $^{***}p < 0.001$.

FIGURE 2 The phenotype of CD83$^+$ CD3$^-$ CD19$^+$B cells and its role in EAU. (a) The gene expression of *CD83, CD40, CD80, CD86, EBI3, IL-10, H2-Aa, H2-D1, H2-Ab1, H2-K1, H2-Eb1* and *CD74* in the CD83$^+$ B cells and CD83$^-$ B cells. (b) The expression of CD40, CD80, CD86 and MHC-II in the CD83$^+$ B cells and CD83$^-$ B cells, and (c) the percentage of IL-10 or IL-35 (IL-12p35) positive CD83$^+$ B cells or CD83$^-$ B cells. (d) Representative images of the retina from a mock mouse, EAU, EAU with CD83$^+$ B cells transfer, EAU$^{\mu mT}$ and EAU$^{\mu mT}$ with CD83$^+$ B cells transfer, as assessed by histology. H&E staining of the retina at 200× magnification. Black arrows mark retinal disorganization. Scale bar = 100 μm. The histopathological scores were evaluated in every mouse group (right panel). (e) The percentage of DCs and CD3$^+$ T cells in the ocular cells of mock mice, EAU, EAU with CD83$^+$ B cells transferring, EAU$^{\mu mT}$ and EAU$^{\mu mT}$ with CD83$^+$ B cells transfer were compared. (f) The percentage of DCs and CD3$^+$ T cells in the lymph node of mock mice, EAU, EAU with CD83$^+$ B cells transfer, EAU$^{\mu mT}$, and EAU$^{\mu mT}$ with CD83$^+$ B cells transfer were compared. (g) The percentage of IFN-γ$^+$CD4$^+$T cells from mock mice, EAU, EAU with CD83$^+$ B cells transferring, EAU$^{\mu mT}$ and EAU$^{\mu mT}$ with CD83$^+$ B cells transfer were compared. (h) Comparison of the concentration of IL-1β, IL-18 and IFN-γ in the serum from EAU and EAU with CD83$^+$ B cells transferring. (i) Percentage of IL-1β, IL-18 and IFN-γ positive in DCs from EAU and EAU with CD83$^+$ B cells transferring. Data are from three separate experiments with five mice/group, and shown as mean ± SEM, data of (a–c), (h) and (i) were analysed by *t*-test. Data of (d, e and f) and (g) were analysed by one-way ANOVA, $^*p < 0.05$, $^{**}p < 0.01$, $^{***}p < 0.001$.

and IFN-γ expression in T cells (Figure S6a,b). After transferring CD83$^+$ B cells in EAU$^{CD11c\text{-}DTR}$ mice, an EAU model established in CD11c-DTR mice (mice with depleted DCs) further decreased the percentage of CD3$^+$ T cells and CD4$^+$ IFN-γ$^+$ T cells (Figure S6c,d). When CD83$^+$ B cells were cocultured with DCs in vitro, CD83$^+$ B cells decreased the expression of CD80, CD86 and CD83 in activated DCs, which were stimulated by IRBP and PTX (Figure 3a), and decreased the secretion of IFN-γ, IL-18 and IL-1β from DCs (Figure 3b). Moreover, CD83$^+$ B cells pre-treated DCs co-cultured with T cells downregulated CD69 and Ki67 expression in T cells (Figure 3c) and decreased the CD4$^+$ IFN-γ$^+$ T cells (Figure 3d). Above all, CD83$^+$ B cells decreased T cells directly or decreased T cells by suppressing DCs in EAU.

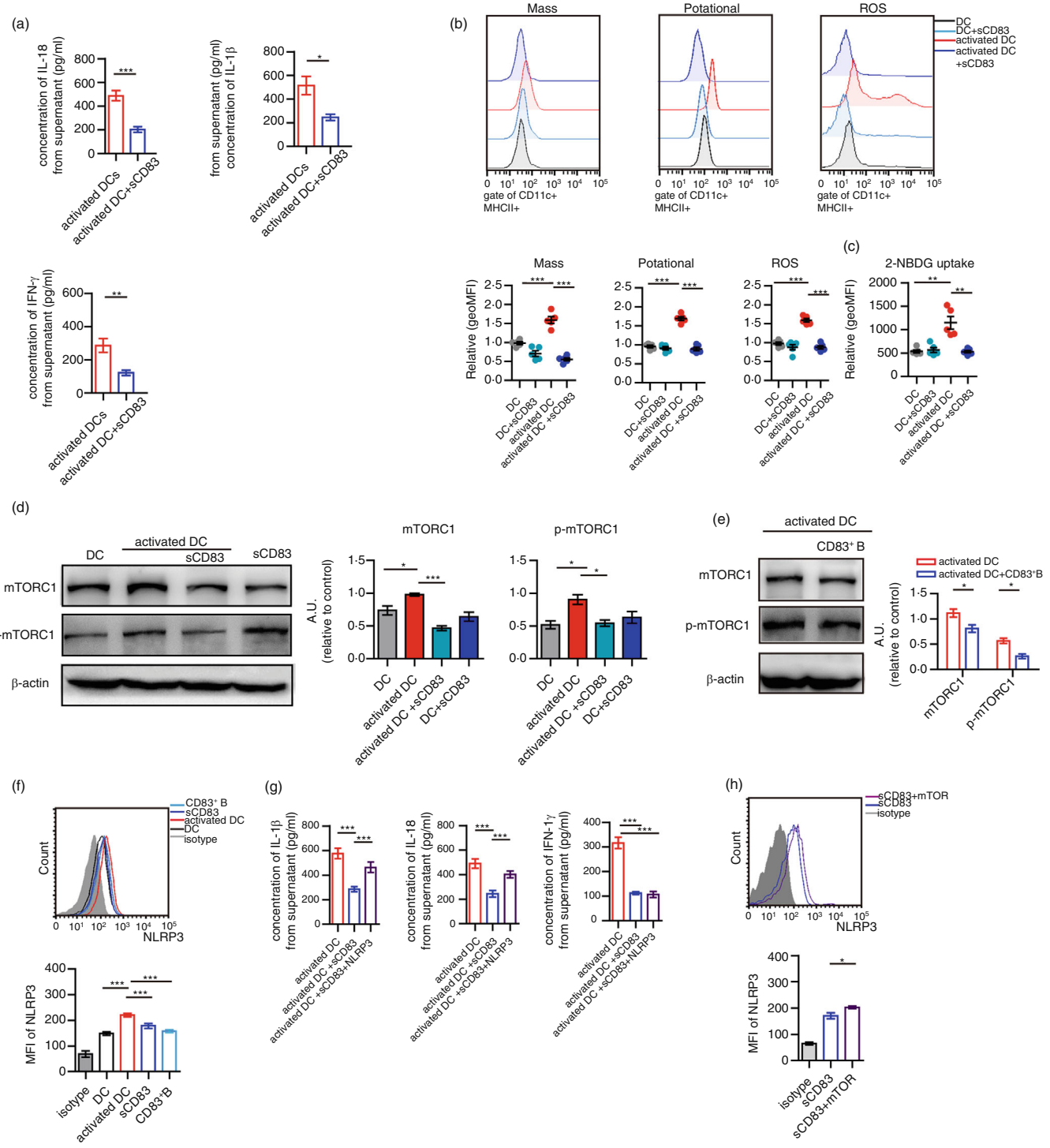

FIGURE 4 Legend on next page.

sCD83 secreted by CD83$^+$ B cells decrease the pro-inflammatory cytokines and the cellular metabolism of DCs

CD83$^+$ B cells could regulate DC through secreting sCD83, so the effect of sCD83 on DC was further studied. Our studying show that sCD83 decreases the secretion of IL-1β, IL-18 and IFN-γ of DCs (Figure 4a). sCD83 decreased the mitochondrial mass, membrane potential, ROS production, and glucose uptake in DCs, especially for activated DCs (Figure 4b,c). Although, the shRNA-CD83 treatment decreased the expression of CD83 on B cells to decrease the production of sCD83, these shRNA-CD83-treated B cells could not influence pro-inflammatory cytokines secretion and the cellular metabolism of DCs (Figure S7a–c), indicating that decreasing the production of sCD83 can eliminate the inhibition of CD83$^+$B cells on DCs.

Moreover, sCD83 targets DCs in EAU via sCD83-YFP protein (Figure S8a). Thus, the inhibition of sCD83 could be on DCs in EAU. Although sCD83 treated DC decreased the activation of CD4$^+$ T cells in vitro [20], sCD83 could not influence the activation and the percentage of IFN-γ$^+$ T cells directly (Figure S8b,c). Thus, the inhibition of sCD83 in EAU might mainly be through the influence of DCs to affect T cells. Above all, sCD83 secreted from CD83$^+$ B cells was an important inhibitor to inhibit the cellular metabolism and the secretion of pro-inflammatory cytokines of DCs in EAU.

sCD83 regulated the cell metabolism and activation of DCs by suppressing the expression phospho (p)-mTORC1 and NLRP3

Furthermore, the mechanism of sCD83 on DCs was detected. mTORC1 is a critical regulator for cell metabolism of DCs [26] and it regulates the activation and function of DCs including IL-1β and IL-18 production [37–39], so the expression of mTORC1 and p-mTORC1 were detected in sCD83 or CD83$^+$ B cells treated DCs. sCD83 treatment reduced the expressions of mTORC1 and p-mTORC1 in activated DCs (Figure 4d). CD83$^+$ B cells treatment also reduced the expression of mTORC1 and p-mTORC1 in activated DCs (Figure 4e).

The expression of NLRP3 was higher in activated DCs than in resting DCs, and sCD83 or CD83$^+$ B cell treatment reduced the expression of NLRP3 in activated DCs (Figure 4f). Overexpression of NLRP3 in DCs reversed the inhibition of sCD83 on the secretion of IL-1β and IL-18 in DCs (Figure 4g). Overexpression of mTOR also reversed the expression of NLRP3 in sCD83-treated DCs (Figure 4h). Thus, sCD83 regulates metabolism and the pro-inflammatory cytokines secretion in activated DCs by mTORC1/ NLRP3 pathway.

sCD83 targeted Rab1a and downregulated its expression by promoting Rab1a accumulation into autolysosomes

The sCD83-GST fusion protein was purified (Figure S9) and used to identify the possible targets of sCD83 in DCs by GST-pull-down plus mass spectrometry (Figure S10). The mass spectrometry results showed that >100 proteins might be binding with sCD83 (Table S1 presents the top 50 proteins). Among the candidate targeted proteins, Rab1a is a small G protein that promotes the phosphorylation of mTORC1-mediated metabolism in cells [40]. Our reports showed that sCD83 treatment decreased Rab1a expression in DCs [41]. Therefore, we further studied the mechanism of sCD83 on Rab1a expression. The *Rab1a* gene was cloned, and the corresponding protein was purified (Figure S11). The GST-pull-down assay confirmed the interaction between sCD83-GST and Rab1a. (Figure 5a,b). In addition, as the concentration of Rab1a increased, the

FIGURE 4 sCD83 affect the cell metabolism and pro-inflammatory factor production in activated DCs by regulating the expression of mTORC1 and NLRP3. (a) The concentration of IL-1β, IL-18 and IFN-γ from the supernatant of DCs + sCD83 (100 ng/mL) or not. (b) Representative histograms (top) and relative expression (bottom) of mitochondrial mass, membrane potential, and ROS production in resting DCs which express low level of CD80, CD86 and MHC-II (DC), activated DCs which were activated by PTX and $IRBP_{20}$ and express high level of CD80, CD86 and MHC-II, and both of with sCD83 treatment, separately (c) Uptake of a fluorescent glucose analogue by resting DCs, activated DCs, and both of with sCD83 treatment, separately. Data of (b, c) are from five separate experiments and shown as mean ± SEM one-way ANOVA，$^*p < 0.05$, $^{***}p < 0.001$. (d) With sCD83 treatment or not, the expression of mTORC1 and p-mTORC1 in resting DCs or activated DCs was detected. (e) The expression of p-mTORC1 and mTORC1 in activated DCs and CD83$^+$ B cells treated activated DCs. (f) The expression of NLRP3 in the DCs, activated DCs, DCs + sCD83, CD83$^+$ B-treated-activated DCs. (g) NLRP3 overexpression rescued the inhibition of sCD83 on pro-inflammatory factor production of IL-1β, IL-18 and IFN-γ from DCs. (h) mTOR over-expression rescued the inhibition of sCD83 on NLRP3 expression of DCs. Data of (a and d–h) are from three separate experiments and shown as mean ± SEM, data of (a, e and h) were analysed by *t*-test; and data of (b–d, f and g) were analysed by one-way ANOVA, $^*p < 0.05$, $^{**}p < 0.01$, $^{***}p < 0.001$.

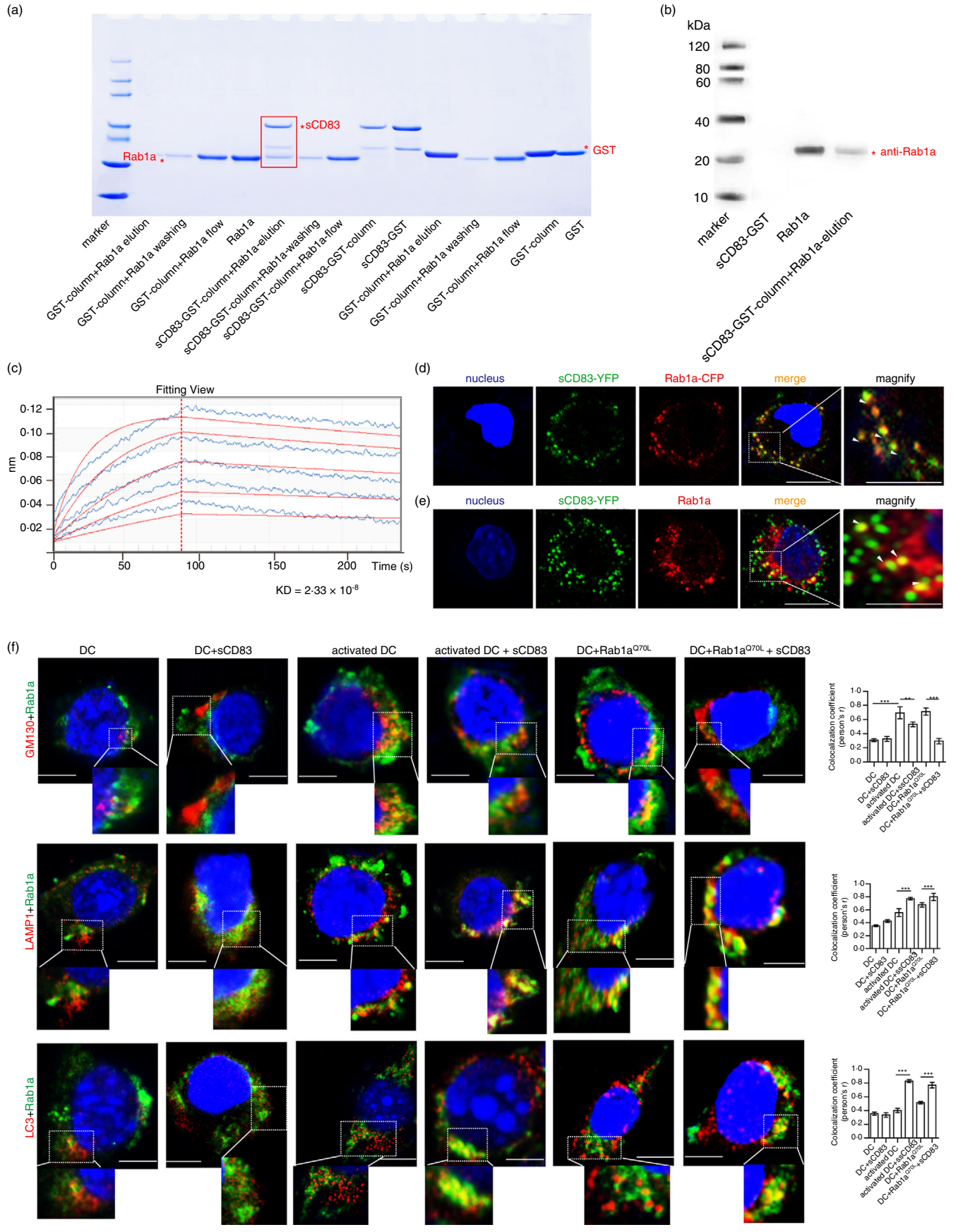

FIGURE 5 Legend on next page.

affinity between sCD83 and Rab1a also increased. The response of the interaction was 0.0309, 0.0514, 0.0655, 0.090, 0.1096, resulting in KD = 2.33×10^{-8} (M) (Figure 5c). Thus, a strong affinity was noted between sCD83 and Rab1a. Furthermore, the direct interaction between sCD83 and Rab1a was examined by confocal microscopy and Förster resonance energy transfer (FRET) analysis. The image analysis showed that sCD83-YFP (green) was colocalized with Rab1a-CFP (red), and FRET was performed (Figure 5d, FRET (p) = 0.0129). In addition, the sCD83-YFP protein was added to the activated DC2.4 cells and incubated for 24 h. The sCD83-YFP (green) was taken up by DC2.4 cells, which were then colocalized with endogenous Rab1a (red) (Figure 5e). Therefore, sCD83 binds to Rab1a to exert its biological effects on cells.

sCD83 bound more with Rab1a-GMP-PNP but not Rab1a-GDP (Figure S12a,b), while only GDP or GMP-PNP could not bind with sCD83-GST. Furthermore, to confirm whether sCD83 tended to bind with activated Rab1a, three mutants, Rab1a^{Q70L} (activated form), Rab1a^{S25N} (inactivated form), and Rab1a^{N124I} (dominant-negative guanine nucleotide-binding deficient mutant) were constructed and pulled down with GST-sCD83, respectively. Notably, more Rab1a^{Q70L} bound with sCD83-GST than other mutants (Figure S12c,d). Moreover, sCD83-YFP preferred colocalizing with Rab1a^{Q70L} than Rab1a^{S25N} or Rab1a^{N124I} in DCs (Figure S12e). Thus, it could be deduced that sCD83 prefers to bind with activated Rab1a.

The localization of Rab1a in the resting and activated DCs with or without sCD83 treatment was detected by immunofluorescence. Rab1a aggregated on the Golgi apparatus (made with GM130) [42] in activated DCs, but it left the Golgi apparatus in sCD83-treated activated DCs (Figure 5f) and co-localized with LAMP1 (a marker of lysosomal) [43] and LC3 (a marker of autophagosome) [44] (Figure 5f). However, no distinct colocalization was detected in the other groups (Figure 5f). In addition, the overexpression of Rab1a^{Q70L} in DCs promoted the accumulation of Rab1a on the Golgi apparatus. Nonetheless, when sCD83 was added to Rab1a^{Q70L}-overexpressing DCs, Rab1a left the Golgi apparatus to co-localize with LAMP1 and LC3 (Figure 5f). Thus, it suggested that sCD83 could promote Rab1a localization and aggregation in autolysosomes.

Rab1a is essential for the function and metabolism of DCs and regulates the effect of sCD83 on DCs

Silencing Rab1a decreased the expression of CD80, CD86 and CD83 and decreased the secretion of IL-1β, IL-18 and IFN-γ on DCs as well (Figures 6a,b and S13a), weakened DC-mediated T cell activation (Figures 6c,d and S13b) and decreased the mitochondrial ROS production, mitochondrial mass, membrane potential and glucose uptake of DCs (Figure 6e). Conversely, the overexpression of Rab1a^{Q70L} upregulated the expression of CD80, CD86, CD83, IL-1β, IL-18 and IFN-γ in DCs (Figures 6a,b and S13a), elevated the function of DCs on activating T cells and the percentage of IFN-γ$^+$ T cells (Figures 6c,d and S13b), and promoted mitochondrial metabolism and glucose uptake in DCs (Figure 6e), compared with the control group. Thus, Rab1a is essential for the function and metabolism of DCs. Furthermore, Rab1a^{Q70L} overexpression rescued the inhibition of sCD83 on the activation and function of DCs on T cells, and mitochondrial metabolism and glucose uptake in DCs (Figures 6f–h and S13c,d). Thus, Rab1a is an essential target of sCD83 for suppressing DC activation and function.

Rab1a increased the expression of mTORC1 and NLRP3 in DCs

The expression of mTORC1 and p-mTORC1 decreased in the shRNA-Rab1a-treated activated DCs (Figure 7a),

FIGURE 5 sCD83 interacts with Rab1a in DCs. (a) sCD83 binding with Rab1a protein was detected by GST-pulldown and analysed by SDS-PAGE. The column alone, GST-bound column, and sCD83-GST-boud column were used to incubate with Rab1a protein. The flowing buffer, washing buffer and elution buffer were used to collect the proteins. The red stars indicated the sCD83 protein, Rab1a protein, and GST protein. (b) Rab1a was detected in the sCD83-GST-Rab1a elution by western blot (WB), Rab1a protein was used as a positive control, and the sCD83-GST fusion protein was used as the negative control. (c) The binding affinity of sCD83 and Rab1a was analysed by bio-layer interferometry. The blue line is background data, and the red line is interaction data. (d) sCD83-YFP (green) and Rab1a-CFP (red) plasmid were co-transfected into the DC2.4 cell line, and their colocalization (yellow) was detected by confocal microscopy. Co-localization index (Pearsons'r) = 0.81 ± 0.04 (mean ± SEM). (e) sCD83-YFP protein (10 ng/mL, green) was used to treat DC2.4 cells for 24 h. Scale bar = 5 μm. The nucleus of (d, e) is blue. Co-localization index (Pearsons'r) = 0.67 ± 0.04 (mean ± SEM). (f) The localization of Rab1a (green) and GM130, or LAMP1, or LC3 (red) in DCs, sCD83-treated-DCs, activated-DCs or sCD83-treated-activated DCs, Rab1a^{Q70L} overexpressed DCs, and sCD83-treated-Rab1a^{Q70L} overexpressed DCs. The nucleus is blue. Co-localization index (Pearsons'r) were graphically represented (right panel) (data from three separated cells). mean ± SEM, data of figure (f) was analysed by one-way ANOVA, ***$p < 0.001$. The nucleus is blue. Scale bar = 5 μm. The dotted box indicates the position of Rab1A contact with Golgi (makered with GM130), lysosome (makered with LAMP1) and autophage (makered with LC3), respectively.

while Rab1a^{Q70L} overexpression promoted p-mTORC1 expression compared with NC-treated activated DCs (Figure 7b). Thus, activated Rab1a is a key protein for the phosphorylation of mTORC1 in DCs. Rab1a^{Q70L} overexpression reversed the suppression of mTORC1 activation in sCD83-treated activated DCs (Figure 7c). Furthermore, sCD83 treatment disrupted the colocalization of Rab1a and p-mTORC1 in activated DCs (Figure 7d). Rab1a^{Q70L} overexpression rescued the disruption of sCD83 on the colocalization of Rab1a and p-mTORC1 in DCs (Figure 7d). Thus, Rab1a played a major role in the effect of sCD83 on the phosphorylation of mTORC1 of DCs.

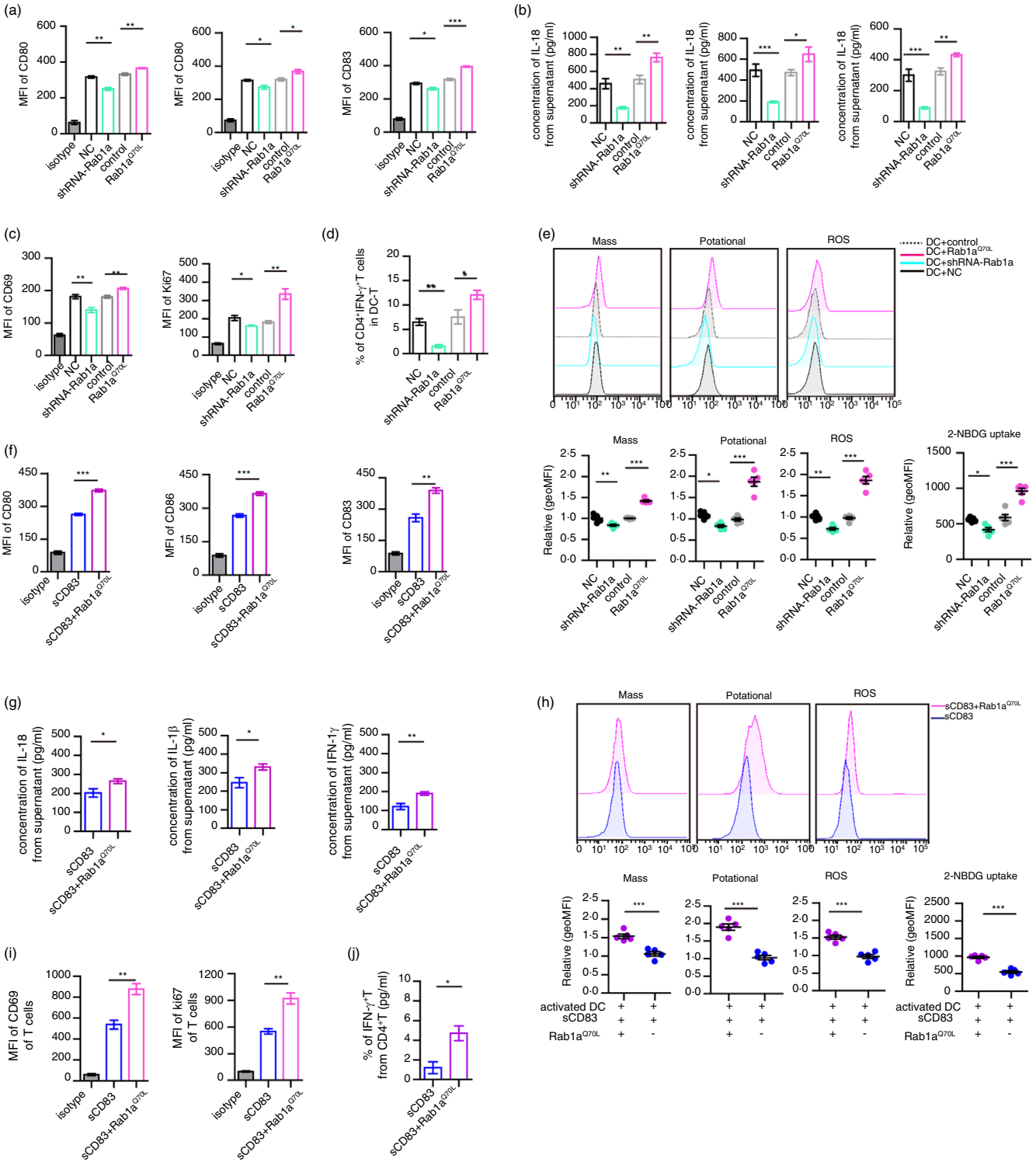

FIGURE 6 Legend on next page.

Silencing Rab1a could decrease the expression of NLRP3 in activated DCs (Figure 7e). Rab1a^{Q70L} overexpression promoted NLRP3 expression compared with the control plasmid-treated activated DCs (Figure 7f). Thus, activated Rab1a is a key protein for expressing NLRP3 in DCs. Rab1a^{Q70L} overexpression rescued the NLRP3 expression in sCD83-treated activated DCs (Figure 7g). When Rab1a^{Q70L} was overexpressed in DC2.4, and the cells were treated with rapamycin to inhibit mTORC1, the NLRP3 inflammasome activation also decreased (Figure 7h). Thus, Rab1a regulated NLRP3 activation by mTORC1. Above all, Rab1a plays an important role in regulating mTORC1 and NLRP3 activation, which influence cellular metabolism and pro-inflammatory factors production of DCs. sCD83 might suppress the activation and function of DCs by inhibiting the Rab1a-mediated mTORC1/NLRP3 pathway.

Expression of CD83$^+$ B cells in Behcet's disease

The uveitis in Behcet's disease (BD) is a type of AIU [45, 46]. Our study showed that the concentration of sCD83 was high in the serum of BD patients, while the levels of IL-10 and IL-35 were not high compared with the healthy individuals (Figure 8a). The concentrations of IL-10, IL-35 and sCD83 in the serum of patients with BD uveitis were lower than in those with acute uveitis (Figure 8a).

The percentage of CD83$^+$ B cells in the blood of BD patients was also increased, but it was lower than in acute uveitis (Figure 8b). Moreover, the expression level of CD83 in B cells from BD patients is lower than that from acute uveitis patients (Figure 8b), which might be correlated with the low concentration of sCD83 in the serum of BD patients compared with those in the serum of acute uveitis. These data indicated that CD83$^+$ B cells and sCD83 were involved in regulating BD, but the deficiency of sCD83 may be an important cause of recurrent BD.

DISCUSSION

The regulatory function and mechanism of B lymphocytes are unclear in uveitis. The B cells participate in experimental and clinical uveitis and exert an inflammatory role in the early stages of the disease [47–50]. Furthermore, mouse models of EAU$^{\mu MT}$, which are defective in functional B cells, had severe symptoms similar to EAU. Although B cells are involved in EAU, B cells are not the only pathogenic factors in this disease. Indeed, Bregs expressing IL-10 and IL-35 were reported to alleviate autoimmune diseases [47]. Although many subsets of Bregs are known, the phenotype of Bregs involved in EAU remains unclear, and the mechanism of Bregs remains to be explored. This study showed that CD83$^+$ CD3$^-$ CD19$^+$ B cells play a regulatory role in uveitis by secreting sCD83, which has not been described in AIU. Silencing CD83 expression leads to decreased secretion of IL-10 and IL-35 in B cells. It is similar to previous reports showing that overexpressed CD83 in B cells inhibited the function of B cells by increasing IL-10 and reducing Ig secretion [51], whereas the deficiency of CD83 in B cells promoted Ig secretion and decreased IL-10 secretion [17, 18]. Thus, CD83 expression was correlated with Bregs function. We also demonstrated that CD83$^+$ CD3$^-$ CD19$^+$ B cells decreased the activation and cellular metabolism of DCs by decreasing Th1 cells to alleviate the symptoms of EAU. CD83$^+$ B cells decreased the secretion of IL-1β, IL-18 and IFN-γ in DCs. IL-18 enhances IFN-γ production and can influence the IFN-γ

FIGURE 6 Rab1a is essential for the membrane CD83 expression, cellular metabolism and pro-inflammatory cytokines of DCs. (a) With shRNA-NC (NC), shRNA-Rab1a, empty plasmid (control) or Rab1a^{Q70L} treatment, representative histograms (upper line) and relative surface expression (bottom line) of CD80, CD86 and CD83 on DCs. (b) The concentration of IL-1β, IL-18 and IFN-γ from the supernatant of DCs with NC, shRNA-Rab1a, control plasmid, or Rab1a^{Q70L} treatment. (c) The expression of CD69 and Ki67 in T cells co-cultured with DCs, which were treated with NC, shRNA-Rab1a, control plasmid, or Rab1a^{Q70L}. (d) The percentage of IFN-γ$^+$ T cells from T cells co-cultured with DCs which were treated with NC, shRNA-Rab1a, control plasmid, or Rab1a^{Q70L}. (e) With NC, shRNA-Rab1a, control plasmid or Rab1a^{Q70L} treatment, representative histograms (upper pannel) and relative expression (bottom pannel) of mitochondrial mass, membrane potential, and ROS production in DCs and uptake a fluorescent glucose analog by DCs. (f) The relative surface expression (bottom line) of CD80, CD86 and CD83 on sCD83-treated activated DCs or Rab1a^{Q70L}overexprssed sCD83-treated activated DCs. (g) The concentration of IL-1β, IL-18 and IFN-γ from DCs with sCD83 or sCD83 and Rab1a^{Q70L} treatment. (h) With Rab1a^{Q70L} treatment or not, representative histograms (upper panel) and relative expression (bottom panel) of mitochondrial mass, membrane potential, and ROS production in sCD83-treated activated DCs and uptake of a fluorescent glucose analog by sCD83-treated activated DCs. (i) The expression of CD69 and Ki67 in T cells with sCD83-treated activated DCs or Rab1a^{Q70L}overexprssed sCD83-treated activated DCs. (j) The percentage of IFN-γ$^+$ T cells from T cells co-cultured with DCs which with sCD83 or sCD83 and Rab1a^{Q70L} treatment. Data of (e, h) are from five separate experiments, and other data are from three separate experiments and shown as mean ± SEM, data of (a–e) were analysed by one-way ANOVA, and data of (f–j) were analysed by *t*-test, $^*p < 0.05$, $^{**}p < 0.01$, $^{***}p < 0.001$.

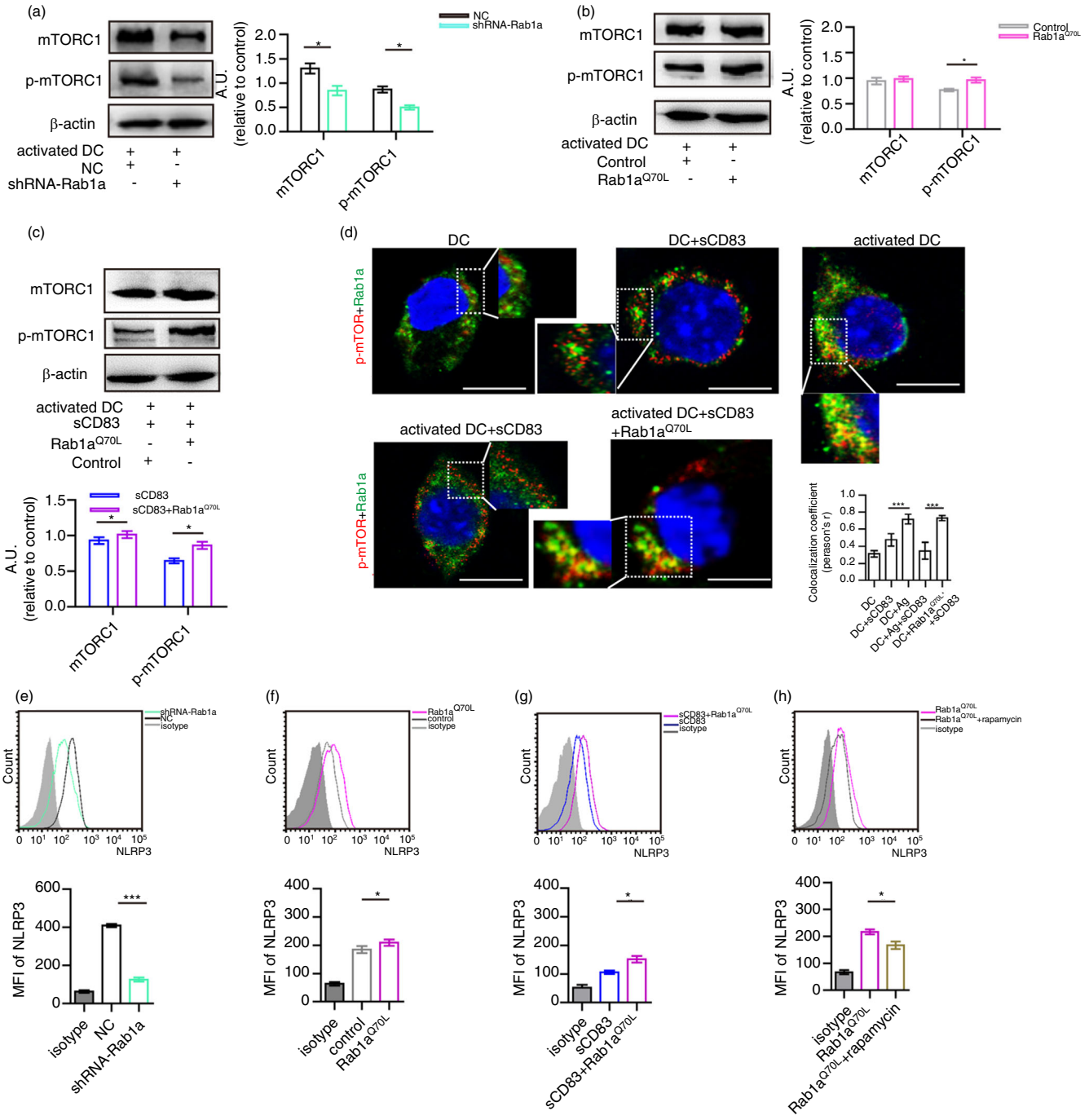

FIGURE 7 Rab1a regulated the expression of mTORC1, p-mTORC1 and NLRP3 in DCs. (a) The expression of mTORC1 and p-mTORC1 in activated DCs with NC or shRNA-Rab1a treatment. (b) The expression of mTORC1 and p-mTORC1 in activated DCs with control plasmid or Rab1a^{Q70L} treatment. (c) With Rab1a^{Q70L} treatment or not, the expression of mTORC1 and p-mTORC1 in sCD83-treated activated DCs. (d) The localization of Rab1a (green) and p-mTORC1 (red) in the DCs, sCD83 treated DCs, activated DCs, sCD83-treated-activated DCs and Rab1a^{Q70L} overexpressed-sCD83-treated-activated DCs. The nucleus is blue. Scale bar = 5 μm. Co-localization index (Pearsons'*r*) were graphically represented (right panel) (data from three separated cells). (e) The expression of NLRP3 in DCs with NC or shRNA-Rab1a treatment. (f) The expression of NLRP3 in DCs with control plasmid or Rab1a^{Q70L} treatment. (g) With Rab1a^{Q70L} treatment or not, the expression of NLRP3 in sCD83-treated activated DCs. (h) With Rab1a^{Q70L} transduction and rapamycin-treated, the expression of NLRP3 in DCs. Data are from three separate experiments and shown as mean ± SEM, data of (a–c) and (e–h) were analysed by *t*-test, and data of (d) was analysed by one-way ANOVA, *$p < 0.05$, **$p < 0.01$, ***$p < 0.001$.

secretion in DCs and T cells [52, 53]. It might be a reason for CD83$^+$ cells relieving the symptoms of EAU. The increased CD83$^+$ CD3$^-$ CD19$^+$ B cells were found in patients with acute uveitis, whereas the percentage of

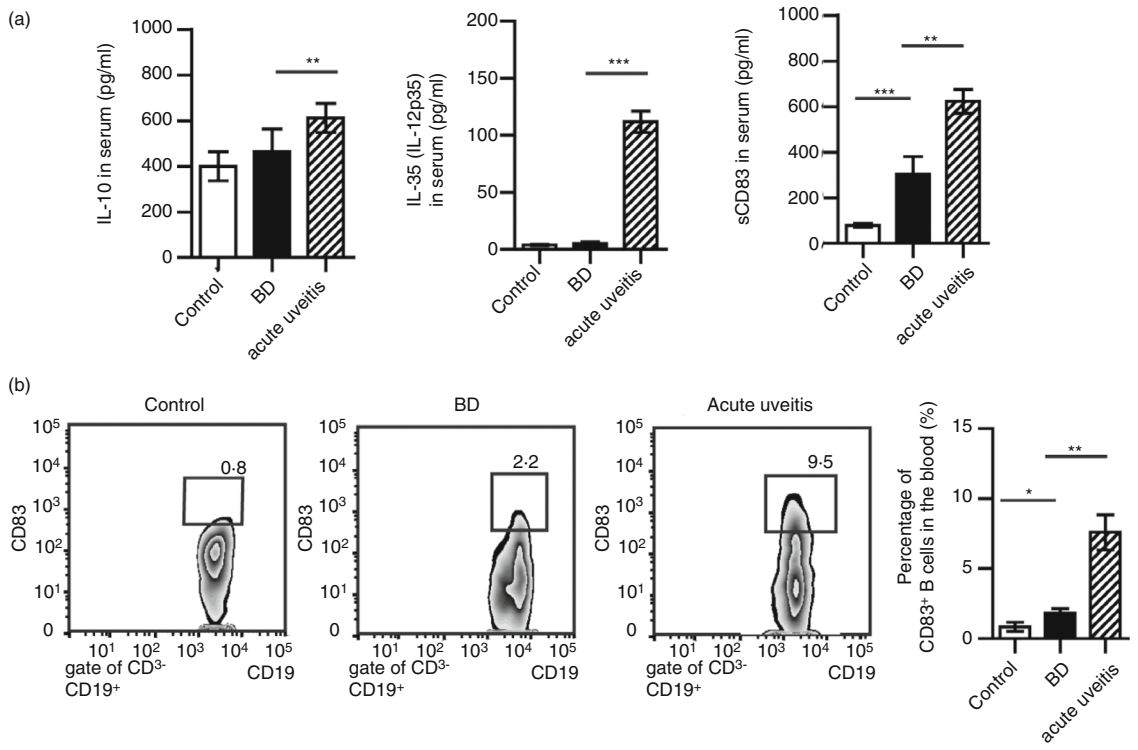

FIGURE 8 The characteristics of sCD83 and CD83$^+$ B cells in the serum of healthy people or with Behcet's disease. (a) Comparison of the concentration of IL-10, IL-35 and sCD83 in the serum of healthy people (Control) and BD patients, and the comparison of these molecules in the serum of acute uveitis. (b) The percentage of CD83$^+$ CD3$^-$ CD19$^+$ B cells in the blood of healthy people (Control), BD patients, and acute uveitis. Data are from 15 healthy people, 5 BD patients and 10 acute uveitis. Data are from five separate experiments. Mean ± SEM, one-way ANOVA, *$p < 0.05$, **$p < 0.01$, ***$p < 0.001$.

CD83$^+$ CD3$^-$ CD19$^+$ B cells in BD was lower than in acute uveitis. Increased CD83$^+$ CD3$^-$ CD19$^+$ B cells might be overregulated in acute disease, whereas a lack of regulation of CD83$^+$ B cells might cause recurrent and refractory BD. Further clinical studies on the reasons for the dysregulation of CD83$^+$ B cells in such diseases need to be investigated.

Unlike previous reports stating that B cells produced IL-10, IL-35, IL-6 or IgGs to influence the function of DCs [54, 55], we found that CD83$^+$ B cells suppressed the activation and metabolism of DCs by producing sCD83. CD83$^+$ B cells have the phenotype of mature B cells and secrete anti-inflammatory factors IL-10, IL-35 and sCD83. IL-35 including its subunit IL-12 p35 preferentially induces expansion of Breg cells and inhibits the activation of DC and pathogenic Th17 and Th1 cells [47, 56, 57]. Our study found that the expression of CD83 in B cells increase the secretion of sCD83, IL-10 and IL-35. sCD83 is the extracellular segment of mCD83 and regulates the adaptive immune response by directly acting on DCs but not influencing the activation of T cells [12]. The secretion of sCD83 by CD83$^+$ B cells might be a new way for B cells to modulate the function of DCs. Moreover, our study further confirmed that CD83$^+$ B cells are primary sources of sCD83, which mainly targeted DCs in EAU. The effect of sCD83 on the regulation of DCs was through the interaction with Rab1a to promote its degradation in autophagosome and inhibit the activation of Rab1a to suppress the mitochondrial metabolism and the activation of DCs (Figure S14). It may be that sCD83 combines with Rab1a after absorbed by DC [58] to promote Rab1a to transfer lysosome from Golgi body and degrade excessive protein through autophagy. Thus, the localization of Rab1a on Golgi apparatus and the activation of mTORC1 are reduced. This effect was seen in activated DCs but not resting DCs, which might be correlated with different expression levels and activation of Rab1a in both cell states. Our study confirmed that the inhibition of CD83$^+$ B cells on DC was partially achieved by sCD83, and whether IL-10 or IL-35 was involved the inhibition of CD83$^+$ B cells remains to be further studied.

Recently, Rab1a has been proven to be an important regulator in the inflammatory response of macrophages and microglial cells [59, 60], but the role of Rab1a in DCs is little known. Rab1a belongs to the small G-proteins family. It promotes and regulates the docking and fusion of transport vesicles and is related to the vesicular transport to the Golgi body, membrane protein expression

[61], skeleton protein movement [62], and the activation of the intracellular signal pathway, including the mTORC1 pathway [40]. The downregulation of Rab1a inhibits cell growth, migration, invasion, and epithelial-mesenchymal transition [63–65]. The inhibition of Rab1a activation also disrupts mitochondrial functions and mTORC1 activation [60, 62, 65, 66]. Moreover, mTORC1 controls the mitochondrial metabolism in DCs [27] and partially influences the Treg expansion and IFN-γ production in DCs [67–69]. Thus, Rab1a regulates the metabolism and function of DC by controlling mTORC1. Because mTOR regulates the activation of the NLRP3 inflammasome partially via ROS-induced NLRP3 expression [38, 70], only inhibiting mTORC1 also inhibited NLRP3 inflammasome activation [71], which cause secretion of interleukin-1β (IL-1β) and IL-18. Thus, mTORC1 could regulate the production of IL-1β and IL-18 by ROS-induced NLRP3 activation (Figure S14). The current study confirmed that the Rab1a-mTORC1 pathway regulated the pro-inflammatory cytokines and proved that this pathway plays a positive regulatory role in DCs, which has never been reported before. Rab1a regulates the cell metabolism and pro-inflammatory factor secretions of DC by modulating the activation of mTORC1 and NLRP3 (Figure S14). However, sCD83 treatment inhibits the pro-inflammatory factor secretions from DCs by decreasing Rab1a expression. Our study provides new insight into the role of Rab1a in the inflammatory response of DC.

The pathogenesis of AIU is still unclear. The levels of IL-10 and IL-35 were not increased in BD patients, which might result from the lack of negative regulation in AIU. The concentration of sCD83 was slightly increased in BD but was lower than in acute uveitis. $CD83^+$ B cells in BD and acute uveitis were low. Lacking enough $CD83^+$ B cells and sCD83 might be involved in BD and AIU. Whether the gene-regulated expression of CD83 or the secretion of sCD83 is a deficiency or the infection factors lead to the decrease of $CD83^+$ B or sCD83 secretion needs to be further studied in the future. These may be the factors leading to this disease. The treatment of autoimmune diseases remains a challenge [4, 72]. The negative regulation of $CD83^+$ B cells in AIU might be a new idea for treating autoimmune diseases.

This study showed that $CD83^+$ B cells are vital regulatory cells in uveitis and suppress the activated DCs and T cells via sCD83. Moreover, sCD83 acts as a negative regulator in DCs by suppressing their metabolism and the secretion of pro-inflammatory factors by promoting the degradation of Rab1a, which influences mTORC1-mediated cell metabolism and NLRP3 inflammasome-mediated cytokine production. The present study provides evidence that Rab1a is a robust regulator of the activation and function of DCs. Finally, the data provide a novel regulatory mechanism in AIU, which helps understand the recurrent attack mechanism of AIU and seek effective treatment for autoimmune diseases.

AUTHOR CONTRIBUTIONS

Wei Lin designed this research and generated the figures and tables, writing, review & editing. Xin Wang and Xunbin Wei investigation, writing-review & editing. Meng Feng performed the animal experiments, western blot, protein purification, immunofluorescence and flow cytometry experiments. Shuping Zhou performed the cell cultures and plasmid extraction. Tingting Liu performed clinical experiments. Minghao Li performed the cell cultures. All authors contributed to the article and approved the submitted version.

ACKNOWLEDGEMENTS

We acknowledge the kind experimental help from Professor Yiwei Chu (Department of Immunology, Shanghai Medical School, Fudan University, Shanghai, China), Professor Hua Tang (Shandong First Medical University & Shandong Academy of Medical Sciences, Jinan, China).

FUNDING INFORMATION

This work was supported by grants from the Natural Science Foundation of China (81500710 and 81601757); the Shandong Key Research and Development Project (2019GSF108189); projects of medical and health technology development program in Shandong province (2019WS186); and the Innovation Project of Shandong Academy of Medical Sciences.

CONFLICT OF INTEREST STATEMENT

The authors declare that the research was conducted in the absence of any commercial or financial relationships that could be construed as a potential conflict of interest.

DATA AVAILABILITY STATEMENT

The data that support the findings of this study are available from the corresponding author upon reasonable request.

ETHICS STATEMENT

All animal experiments were reviewed and approved by the Experimental Animal Committee of the Shandong First University & Shandong Academy of Medical Sciences (Jinan, China, SYXK20180007). Patients were recruited from the Shandong ophthalmic hospital, and informed consent was obtained. The Human Research and Ethics Committee of Shandong Eye Hospital, Shandong Eye Institute, Shandong First Medical University

and Shandong Academy of Medical School (2019-G-012) granted ethical approval for the study.

ORCID

Wei Lin https://orcid.org/0000-0002-1102-2550

REFERENCES

1. Caspi RR, Roberge FG, McAllister CG, el-Saied M, Kuwabara T, Gery I, et al. T cell lines mediating experimental autoimmune uveoretinitis (EAU) in the rat. J Immunol. 1986; 136(3):928–33.
2. Ilhan F, Demir T, Turkcuoglu P, Turgut B, Demir N, Godekmerdan A. Th1 polarization of the immune response in uveitis in Behcet's disease. Can J Ophthalmol. 2008;43(1): 105–8.
3. Muhaya M, Calder VL, Towler HM, Jolly G, McLauchlan M, Lightman S. Characterization of phenotype and cytokine profiles of T cell lines derived from vitreous humour in ocular inflammation in man. Clin Exp Immunol. 1999;116(3):410–4.
4. Durrani OM, Tehrani NN, Marr JE, Moradi P, Stavrou P, Murray PI. Degree, duration, and causes of visual loss in uveitis. Br J Ophthalmol. 2004;88(9):1159–62.
5. Heuss ND, Lehmann U, Norbury CC, McPherson SW, Gregerson DS. Local activation of dendritic cells alters the pathogenesis of autoimmune disease in the retina. J Immunol. 2012;188(3):1191–200.
6. O'Rourke M, Fearon U, Sweeney CM, Basdeo SA, Fletcher JM, Murphy CC, et al. The pathogenic role of dendritic cells in non-infectious anterior uveitis. Exp Eye Res. 2018;173:121–8.
7. Oh K, Kim YS, Lee DS. Maturation-resistant dendritic cells ameliorate experimental autoimmune uveoretinitis. Immune Netw. 2011;11(6):399–405.
8. Ture-Ozdemir F, Tulunay A, Elbasi MO, Tatli I, Maurer AM, Mumcu G, et al. Pro-inflammatory cytokine and caspase-1 responses to pattern recognition receptor activation of neutrophils and dendritic cells in Behcet's disease. Rheumatology (Oxford). 2013;52(5):800–5.
9. Xu H, Dawson R, Forrester JV, Liversidge J. Identification of novel dendritic cell populations in normal mouse retina. Invest Ophthalmol Vis Sci. 2007;48(4):1701–10.
10. Sokolov AV, Shmidt AA, Lomakin YA. B cell regulation in autoimmune diseases. Acta Nat. 2018;10(3):11–22.
11. Yang M, Rui K, Wang S, Lu L. Regulatory B cells in autoimmune diseases. Cell Mol Immunol. 2013;10(2):122–32.
12. Lin W, Buscher K, Wang B, Fan Z, Song N, Li P, et al. Soluble CD83 alleviates experimental autoimmune uveitis by inhibiting filamentous actin-dependent calcium release in dendritic cells. Front Immunol. 2018;9:1567.
13. Karampoor S, Zahednasab H, Etemadifar M, Keyvani H. The levels of soluble forms of CD21 and CD83 in multiple sclerosis. J Neuroimmunol. 2018;320:11–4.
14. Kristensen AM, Stengaard-Pedersen K, Hetland ML, Hørslev-Petersen K, Junker P, Østergaard M, et al. Expression of soluble CD83 in plasma from early-stage rheumatoid arthritis patients is not modified by anti-TNF-alpha therapy. Cytokine. 2018;96:1–7.
15. Hock BD, O'Donnell JL, Taylor K, Steinkasserer A, McKenzie JL, Rothwell AG, et al. Levels of the soluble forms of CD80, CD86, and CD83 are elevated in the synovial fluid of rheumatoid arthritis patients. Tissue Antigens. 2006;67(1): 57–60.
16. Hock BD, Kato M, McKenzie JL, Hart DN. A soluble form of CD83 is released from activated dendritic cells and B lymphocytes, and is detectable in normal human sera. Int Immunol. 2001;13(7):959–67.
17. Kretschmer B, Luthje K, Schneider S, Fleischer B, Breloer M. Engagement of CD83 on B cells modulates B cell function in vivo. J Immunol. 2009;182(5):2827–34.
18. Luthje K, Kretschmer B, Fleischer B, Breloer M. CD83 regulates splenic B cell maturation and peripheral B cell homeostasis. Int Immunol. 2008;20(8):949–60.
19. Royzman D, Andreev D, Stich L, Rauh M, Bäuerle T, Ellmann S, et al. Soluble CD83 triggers resolution of arthritis and sustained inflammation control in IDO dependent manner. Front Immunol. 2019;10:633.
20. Lin H, Liang S, Zhong Z, Wen J, Li W, Wang L, et al. Soluble CD83 inhibits human monocyte differentiation into dendritic cells in vitro. Cell Immunol. 2014;292(1–2):25–31.
21. Buck MD, Sowell RT, Kaech SM, Pearce EL. Metabolic instruction of immunity. Cell. 2017;169(4):570–86.
22. Pearce EJ, Everts B. Dendritic cell metabolism. Nat Rev Immunol. 2015;15(1):18–29.
23. Zhou R, Yazdi AS, Menu P, Tschopp J. A role for mitochondria in NLRP3 inflammasome activation. Nature. 2011; 469(7329):221–5.
24. Arnoult D, Soares F, Tattoli I, Girardin SE. Mitochondria in innate immunity. EMBO Rep. 2011;12(9):901–10.
25. Krawczyk CM, Holowka T, Sun J, Blagih J, Amiel E, DeBerardinis RJ, et al. Toll-like receptor-induced changes in glycolytic metabolism regulate dendritic cell activation. Blood. 2010;115(23):4742–9.
26. Sukhbaatar N, Hengstschlager M, Weichhart T. mTOR-mediated regulation of dendritic cell differentiation and function. Trends Immunol. 2016;37(11):778–89.
27. Wang Y, Huang G, Zeng H, Yang K, Lamb RF, Chi H. Tuberous sclerosis 1 (Tsc1)-dependent metabolic checkpoint controls development of dendritic cells. Proc Natl Acad Sci U S A. 2013;110(50):E4894–903.
28. Blair J, Barry R, Moore DJ, Denniston AK. A comprehensive review of mTOR-inhibiting pharmacotherapy for the treatment of non-infectious uveitis. Curr Pharm Des. 2017;23(20): 3005–14.
29. Avichezer D, Liou GI, Chan CC, Lewis GM, Wiggert B, Donoso LA, et al. Interphotoreceptor retinoid-binding protein (IRBP)-deficient C57BL/6 mice have enhanced immunological and immunopathogenic responses to IRBP and an altered recognition of IRBP epitopes. J Autoimmun. 2003;21(3):185–94.
30. Avichezer D, Silver PB, Chan CC, Wiggert B, Caspi RR. Identification of a new epitope of human IRBP that induces autoimmune uveoretinitis in mice of the H-2b haplotype. Invest Ophthalmol Vis Sci. 2000;41(1):127–31.
31. Thurau SR, Chan CC, Nussenblatt RB, Caspi RR. Oral tolerance in a murine model of relapsing experimental autoimmune uveoretinitis (EAU): induction of protective tolerance in primed animals. Clin Exp Immunol. 1997;109(2):370–6.
32. Harimoto K, Ito M, Karasawa Y, Sakurai Y, Takeuchi M. Evaluation of mouse experimental autoimmune uveoretinitis by

spectral domain optical coherence tomography. Br J Ophthalmol. 2014;98(6):808–12.
33. Zhao Y, Wang J, Min Z, Peng L, Qi S, Lin W. I-a(low)CD11b (high) DC regulates the immune response in the eyes of experimental autoimmune uveitis. Mediators Inflamm. 2020;2020: 6947482.
34. Li H, Zhu L, Wang R, Xie L, Ren J, Ma S, et al. Aging weakens Th17 cell pathogenicity and ameliorates experimental autoimmune uveitis in mice. Protein. Cell. 2021;13:422–45.
35. Butler A, Hoffman P, Smibert P, Papalexi E, Satija R. Integrating single-cell transcriptomic data across different conditions, technologies, and species. Nat Biotechnol. 2018;36(5):411–20.
36. International team for the revision of the international criteria for Behcet's D. the international criteria for Behcet's disease (ICBD): a collaborative study of 27 countries on the sensitivity and specificity of the new criteria. J Eur Acad Dermatol Venereol. 2014;28(3):338–47.
37. Jia X, Cao B, An Y, Zhang X, Wang C. Rapamycin ameliorates lipopolysaccharide-induced acute lung injury by inhibiting IL-1beta and IL-18 production. Int Immunopharmacol. 2019;67: 211–9.
38. Li X, Zhang X, Pan Y, Shi G, Ren J, Fan H, et al. mTOR regulates NLRP3 inflammasome activation via reactive oxygen species in murine lupus. Acta Biochim Biophys Sin. 2018;50(9): 888–96.
39. Huang XH, Ma Y, Zheng MM, Chen N, Hu MN, Wu LY, et al. NLRP3 and mTOR reciprocally regulate macrophage Phagolysosome formation and acidification against Vibrio vulnificus infection. Front Cell Dev Biol. 2020;8:587961.
40. Thomas JD, Zhang YJ, Wei YH, Cho JH, Morris LE, Wang HY, et al. Rab1A is an mTORC1 activator and a colorectal oncogene. Cancer Cell. 2016;30(1):181–2.
41. Lin W, Zhou S, Feng M, Yu Y, Su Q, Li X. Soluble CD83 regulates dendritic cell-T cell immunological synapse formation by disrupting Rab1a-mediated F-Actin rearrangement. Front Cell Dev Biol. 2021;8:605713.
42. Yang C, Chen N, Li X, Lu D, Hou Z, Li Y, et al. Mutations in the coat complex II component SEC23B promote colorectal cancer metastasis. Cell Death Dis. 2020;11(3):157.
43. Labadie T, Roy P. A non-enveloped arbovirus released in lysosome-derived extracellular vesicles induces super-infection exclusion. PLoS Pathog. 2020;16(10):e1009015.
44. Shao Z, Ni L, Hu S, Xu T, Meftah Z, Yu Z, et al. RNA-binding protein HuR suppresses senescence through Atg7 mediated autophagy activation in diabetic intervertebral disc degeneration. Cell Prolif. 2021;54(2):e12975.
45. Saadoun D, Wechsler B. Behcet's disease. Orphanet J Rare Dis. 2012;7:20.
46. Ksiaa I, Abroug N, Kechida M, Zina S, Jelliti B, Khochtali S, et al. Eye and Behcet's disease. J Fr Ophtalmol. 2019;42(4): e133–e46.
47. Dambuza IM, He C, Choi JK, Yu CR, Wang R, Mattapallil MJ, et al. IL-12p35 induces expansion of IL-10 and IL-35-expressing regulatory B cells and ameliorates autoimmune disease. Nat Commun. 2017;8(1):719.
48. Xu C, Ricciuti A, Caturegli P, Keene CD, Kargi AY. Autoimmune lymphocytic hypophysitis in association with autoimmune eye disease and sequential treatment with infliximab and rituximab. Pituitary. 2015;18(4):441–7.
49. Lund FE, Garvy BA, Randall TD, Harris DP. Regulatory roles for cytokine-producing B cells in infection and autoimmune disease. Curr Dir Autoimmun. 2005;8:25–54.
50. Fujino Y, Li Q, Chung H, Hikita N, Nussenblatt RB, Gery I, et al. Immunopathology of experimental autoimmune uveoretinitis in primates. Autoimmunity. 1992;13(4):303–9.
51. Kretschmer B, Luthje K, Guse AH, Ehrlich S, Koch-Nolte F, Haag F, et al. CD83 modulates B cell function in vitro: increased IL-10 and reduced Ig secretion by CD83Tg B cells. PLoS One. 2007;2(8):e755.
52. Lamkanfi M, Dixit VM. Mechanisms and functions of inflammasomes. Cell. 2014;157(5):1013–22.
53. Stoll S, Jonuleit H, Schmitt E, Muller G, Yamauchi H, Kurimoto M, et al. Production of functional IL-18 by different subtypes of murine and human dendritic cells (DC): DC-derived IL-18 enhances IL-12-dependent Th1 development. Eur J Immunol. 1998;28(10):3231–9.
54. Zietara N, Lyszkiewicz M, Krueger A, Weiss S. B-cell modulation of dendritic-cell function: signals from the far side. Eur J Immunol. 2013;44(1):23–32.
55. Bayry J, Lacroix-Desmazes S, Kazatchkine MD, Hermine O, Tough DF, Kaveri SV. Modulation of dendritic cell maturation and function by B lymphocytes. J Immunol. 2005;175(1): 15–20.
56. Wang RX, Yu CR, Dambuza IM, Mahdi RM, Dolinska MB, Sergeev YV, et al. Interleukin-35 induces regulatory B cells that suppress autoimmune disease. Nat Med. 2014;20(6): 633–41.
57. Jiang H, Li Z, Yu L, Zhang Y, Zhou L, Wu J, et al. Immune phenotyping of patients with acute Vogt-Koyanagi-Harada syndrome before and after glucocorticoids therapy. Front Immunol. 2021;12:659150.
58. Yang Y, Xin Z, Chu J, Li N, Sun T. Involvement of Caveolin-1 in CD83 internalization in mouse dendritic cells. Cell Transplant. 2015;24(7):1395–404.
59. Song S, Pan Y, Li H, Zhen H. MiR-1202 exerts neuroprotective effects on OGD/R induced inflammation in HM cell by negatively regulating Rab1a involved in TLR4/NF-kappaB signaling pathway. Neurochem Res. 2020;45(5):1120–9.
60. Zhang Y, Wang L, Lv Y, Jiang C, Wu G, Dull RO, et al. The GTPase Rab1 is required for NLRP3 Inflammasome activation and inflammatory lung injury. J Immunol. 2019;202(1): 194–206.
61. Yoo JS, Moyer BD, Bannykh S, Yoo HM, Riordan JR, Balch WE. Non-conventional trafficking of the cystic fibrosis transmembrane conductance regulator through the early secretory pathway. J Biol Chem. 2002;277(13):11401–9.
62. Kicka S, Shen Z, Annesley SJ, Fisher PR, Lee S, Briggs S, et al. The LRRK2-related Roco kinase Roco2 is regulated by Rab1A and controls the actin cytoskeleton. Mol Biol Cell. 2011;22(13): 2198–211.
63. Cheng Z, Shao X, Xu M, Wang J, Kuai X, Zhang L, et al. Rab1A promotes proliferation and migration abilities via regulation of the HER2/AKT-independent mTOR/S6K1 pathway in colorectal cancer. Oncol Rep. 2019;41(5):2717–28.
64. Segawa K, Tamura N, Mima J. Homotypic and heterotypic trans-assembly of human Rab-family small GTPases in reconstituted membrane tethering. J Biol Chem. 2019;294(19): 7722–39.

65. Xu H, Qian M, Zhao B, Wu C, Maskey N, Song H, et al. Inhibition of RAB1A suppresses epithelial-mesenchymal transition and proliferation of triple-negative breast cancer cells. Oncol Rep. 2017;37(3):1619–26.
66. Feng ZZ, Jiang AJ, Mao AW, Feng Y, Wang W, Li J, et al. The salmonella effectors SseF and SseG inhibit Rab1A-mediated autophagy to facilitate intracellular bacterial survival and replication. J Biol Chem. 2018;293(25):9662–73.
67. O'Brien A, Loftus RM, Pisarska MM, et al. Obesity reduces mTORC1 activity in mucosal-associated invariant T cells, driving defective metabolic and functional responses. J Immunol. 2019;202(12):3404–11.
68. Wang Y, Du X, Wei J, et al. LKB1 orchestrates dendritic cell metabolic quiescence and anti-tumor immunity. Cell Res. 2019;29(5):391–405.
69. Pelgrom LR, Patente TA, Sergushichev A, Esaulova E, Otto F, Ozir-Fazalalikhan A, et al. LKB1 expressed in dendritic cells governs the development and expansion of thymus-derived regulatory T cells. Cell Res. 2019;29(5):406–19.
70. Cunningham JT, Rodgers JT, Arlow DH, Vazquez F, Mootha VK, Puigserver P. mTOR controls mitochondrial oxidative function through a YY1-PGC-1alpha transcriptional complex. Nature. 2007;450(7170):736–40.
71. Yang F, Ye XJ, Chen MY, Li HC, Wang YF, Zhong MY, et al. Inhibition of NLRP3 Inflammasome activation and Pyroptosis in macrophages by taraxasterol is associated with its regulation on mTOR signaling. Front Immunol. 2021;12:632606.
72. Kempen JH, Altaweel MM, Holbrook JT, Jabs DA, Sugar EA. The multicenter uveitis steroid treatment trial: rationale, design, and baseline characteristics. Am J Ophthalmol. 2010;149(4):550–61 e10.

SUPPORTING INFORMATION

Additional supporting information can be found online in the Supporting Information section at the end of this article.

How to cite this article: Feng M, Wang X, Zhou S, Li M, Liu T, Wei X, et al. CD83$^+$ B cells alleviate uveitis through inhibiting DCs by sCD83. Immunology. 2023;170(1):134–53. https://doi.org/10.1111/imm.13654